VALIDATION OF POWER SYSTEM TRANSIENT STABILITY RESULTS

BY

KOMAL SUDHIR SHETYE

THESIS

Submitted in partial fulfillment of the requirements
for the degree of Master of Science in Electrical and Computer Engineering
in the Graduate College of the
University of Illinois at Urbana-Champaign, 2011

Urbana, Illinois

Adviser:

Professor Thomas J. Overbye

Abstract

Simulation of the transient stability problem of a power system, which is the assessment of the short term angular and voltage stability of the system following a disturbance, is of vital importance. It is widely known in the industry that different transient stability packages can give substantially different results for the same (or at least similar) system models. The goal of this work is to develop validation methodologies for different transient stability software packages with a focus on Western Electricity Coordinating Council (WECC) system models. We discuss two specific approaches developed and implemented to validate the transient stability results. The sources of discrepancies seen in the results from different packages are investigated. This enables us to identify the differences in the implementation of dynamic models in different transient stability softwares. In this process, we present certain key analyses of the WECC system models for different contingencies.

Dedicated with loving memory to my father, Sudhir L. Shetye (1949-2011)

Acknowledgments

I am deeply thankful to my adviser, Professor Thomas Overbye, for his kindness, guidance, support, significant contributions to this work and his immense patience with the time it took me to complete this thesis.

This thesis is based on the Power System Engineering Research Center (PSERC) project entitled “Validation and Accreditation of Transient Stability Results” (Project S43-G). I am grateful to PSERC’s industry member, the Bonneville Power Administration (BPA), for funding this work. I thank Jim Gronquist from BPA for providing valuable support and guidance in this research. I would also like to thank PowerWorld Corporation and GE for all the technical support provided in this work.

I express deep gratitude towards my parents, especially my father who always inspired me to pursue excellence in academics and lead a successful career. I am thankful to my mother, Shakuntala Shetye, for her all her love and support.

Last but not the least, I would like to thank Jay and Ruchika, who have been like my family in Urbana and who have played a major role in helping me reach this milestone.

Table of Contents

1. Introduction

1.1 Motivation and Problem Overview

Simulation of the transient stability problem, which is the assessment of the short term (several to 30 seconds) angular and voltage stability of the power system following a disturbance, is of vital importance. For some portions of the North American power grids, such as Western Electricity Coordinating Council (WECC), transient stability has always been an important consideration, while for other portions, it is of growing concern due partially to the widespread integration of wind generation.

It is widely known that different industry-grade transient stability simulation tools can give substantially different results for the same or at least similar system models. The goal of this thesis is to develop validation methodologies for different transient stability software packages with a focus on WECC system models.

For validation within the power system transient stability domain, there is usually a lack of real-world data to allow a direct comparison between the simulation results and the real world. Rather in this work the main task is to simulate the WECC power system models using different commercial transient stability packages, and use them to "validate" each other. This process will be aided by the fact that all the packages claim to implement the same system models.

1.2 Literature Review

Power system transient stability is essentially the ability of the power system to maintain synchronism when subjected to a severe transient disturbance such as a fault on transmission facilities, loss of generation, or loss of a large load. The system response to such disturbances involves large excursions of generator rotor angles, power flows, bus voltages and other system variables [1]. There are papers that provide limited comparison between various model implementations for different software packages. In [2], benchmarked results for two realistic test systems are provided using the EPRI-Extended Transient/Mid-Term Stability Program (EMSTP) and PTI-Power System Simulation/E Program (PSSE). Although the two systems are chosen to show a wide range of dynamic

characteristics in terms of the mode of instability, they include only two types of machine models, namely the classical model and the two axis model with exciters. The actual number of the types of these models in the WECC system is far more. In [3], the authors evaluate more transient stability software packages such as DIgSILENT, PSSE, and PSCAD on the basis of the power system component models available in each tool and their user-friendliness. However, only a limited number of component models such as synchronous generator, generator saturation, transmission line representation and external network are compared and only one simplified test case is used. K. K. Kabere et al. investigate the turbo-generator modeling employed by five industrial-grade power system simulation tools (PSSE, PowerFactory, EUROSTAG, SSAT and MatNetEig) in their application for small-signal stability analysis [4]. From the disparities in the results obtained from simulating the same system in different tools, the authors conclude that validation of results obtained from different small-signal analysis tools with field experiments is crucial, as is the necessity of benchmarking and standardization of requirements for different simulation tools. In [5], validation of different softwares such as PSSE, DIgSILENT, EUROSTAG and Matlab's Power System Toolbox (PST) was performed with a focus on small-signal stability. Again, here the focus was on generator modeling and solution methodologies. In [6], steady-state performance and the impact of a three-phase transient disturbance were used as the basis for comparisons between some softwares that allow HVDC lines to be modeled, namely DigSILENT, Matlab PST and PSAT. An important conclusion drawn from this work was that the steady state analysis results were similar, especially for the more established and widely used packages like PSSE and DigSILENT. Even in the packages that we are considering in our work such as PowerWorld Simulator, PSSE and GE's Positive Sequence Load Flow program (PSLF), owing to their long history of use of power flow analysis, we expected and correctly encountered a good agreement between the packages with respect to their static network solutions. Since the initialization of a transient stability simulation is based on the steady state network solution, this key fact enabled us to validate our transient stability results more effectively, and any discrepancies in the results from these comparisons could thus be attributed majorly to the dynamic simulation solution.

There are a number of industry and IEEE approved generator, exciter, stabilizer, governor, load and other models that are used in transient stability studies. Some of these models have slightly different representations in different transient stability software packages [7], [8], [9]. This work focuses only on the models used most commonly in the WECC system. Reference [7] contains an extensive library of such models used commonly in industry, a subset of which was analyzed in this work.

1.3 Related Project

This thesis is based on a project funded by the Bonneville Power Administration (BPA), which falls under the purview of WECC. This work was conducted through the Power Systems Engineering Research Center (PSERC). The goal of this project was to enhance the utilization of the BPA transmission system by using validated, real-time transient stability analysis results, and to have better planning/study tools and models. We also provided benchmarked cases and results to BPA to aid their simulation studies on their interconnected power system. This thesis describes the validation studies performed using PowerWorld, PSSE and PSLF. In this project, we received three different versions of the complete WECC power system model comprising roughly 17,000 buses and 3000 generators in PSLF format, and one in the PSSE format. Each successive PSLF case was an improved and updated one. We converted these files to PowerWorld binary files (*.pwb) for the ease of our studies across different packages. In this thesis, we will refer to the case files by the following names:

1. WECC Case 1: PSLF format

2. WECC Case 2: PSLF format

   This updated case, received on June 28 2010, fixed some 2000 errors in the previous version

3. WECC Case 3: PSSE format

   This was the only WECC case received in the PSSE format, in December 2010.

4. WECC Case 4: PSLF format

This was the most recent and updated case provided to us.

Following the WECC standard, a time step of ¼ cycle was used in all the simulations, unless specified otherwise.

The single machine infinite bus (SMIB) cases analyzed in this work were derived from specific buses from the full WECC model. The generator buses from which these equivalents were derived are mentioned in this thesis.

In order to ensure confidentiality of the WECC system data, alternative bus numbers, area names, etc., have been assigned in this thesis, which do not reflect, in any way, the actual numbers or names of any part of the system. This is also the reason why we have maintained ambiguity about locations and names of components such as generating units.

1.4 Thesis Organization

The organization of the thesis is as follows. Chapter 2 describes the detection and correction of bad dynamic model data that we encountered in the full WECC model, and the principles of time-step and auto-correction. Chapter 3 charts out the first aspect of our validation methodology, i.e. the top-down approach, and eventually highlights the significance of SMIB equivalents in the debugging process. Chapter 4 covers the bottom-up approach to validation in some detail, wherein we use SMIB equivalents to validate the major generator models. Chapter 5 discusses validation of generator saturation and exciters with results for the full WECC case, provided by BPA. Chapter 6 provides an insight into time step comparison of results. Chapter 7 describes the latest runs being done on Case 4, some comparison results and the issues encountered. Lastly, Chapter 8 summarizes this work and gives directions for future research.

2. Detection and Correction of "Bad" Data

2.1 Background

The "Run Validation" option in the Transient Stability module of PowerWorld allows the user to check for any data imperfections prior to running a transient stability simulation. The "Validation Errors" essentially are a list of parameters that depict non-physical scenarios or those which might cause the simulation to be numerically unstable or compromise accuracy. Suggestions for auto-correcting some of these parameters are made by PowerWorld, when these errors are encountered. Quite a few of such errors were found in the WECC full cases, which were reported to BPA. Detecting the errors thus made vast improvements in the WECC model. The following sections throw light on this detection and correction of "bad" data.

2.2 Correction of Bad Saturation Data

Magnetic saturation affects the various mutual and leakage inductances within a machine, except the classical generator (GENCLS) model [8]. Saturation data for a machine is entered by specifying the values of two parameters $S(1.0)$ and $S(1.2)$, which are defined in Figure 2.1. It is a known fact that magnetic material saturates with higher flux. Therefore the value of $S(1.2)$ can never be less than the value of $S(1.0)$.

For WECC Case 2, the saturation data for about 28 generators failed to meet the criteria $S(1.2) >= S(1.0)$. This was detected in the PowerWorld validation run.

The suggested auto-correction was to swap the values of $S(1.0)$ with $S(1.2)$.

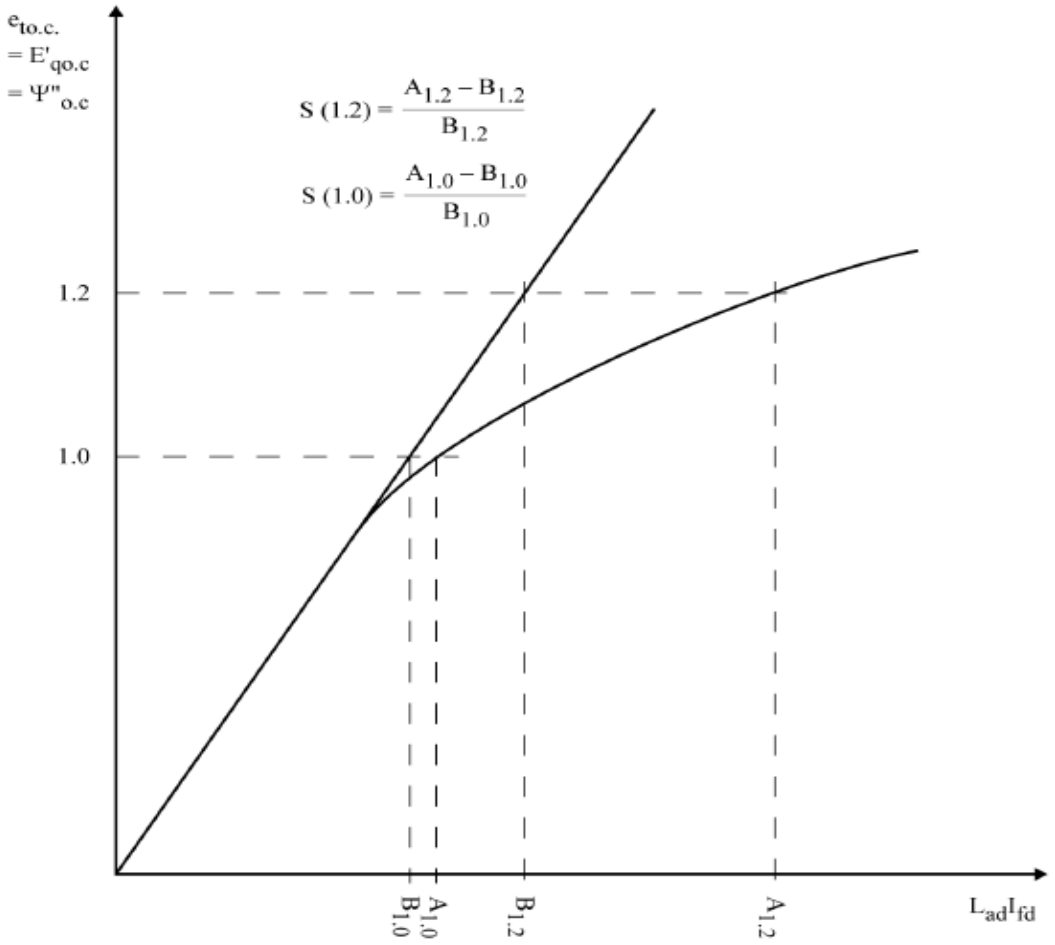

Figure 2.1: Definition of saturation factor, *S*, for entry and generator data [8]

2.3 Machine Impedance Values

The validation of dynamics data associated with a particular model is important in our validation studies. For a generator machine model, this data includes parameters such as inertia constant, stator resistance, transient and sub-transient reactances and time constants, saturation and impedance values of the compensation circuit (if applicable).

In the aforementioned WECC case, we also found some incorrect reactance values. For instance, we found for about 75 generators, the stator leakage reactance X_l was more than the sub-transient direct or quadrature axis reactance, X_{dpp} or X_{qpp}. This is clearly not physically possible for a synchronous machine model, as explained in Equation 4.41 of [1].

2.4 Correction of Time Constants

Setting the appropriate time step is important from the point of view of accuracy and numerical stability of the simulation. Time step is specified either in seconds or a fraction of one cycle. The nominal system frequency for the power system used in our study is 60 cycles per second. As recommended by BPA to follow the WECC standard, a time step of ¼ cycle has been used all throughout this work to conduct all the transient stability simulations, unless specified otherwise.

From Equations 11.3 to 11.7 of [8], it is clear that the numerical integration process in a dynamic simulation can be accurate and stable only if the time step Δt is small in comparison to the time constants used in the simulation; otherwise the integration process might develop an error that grows unstably [8].

PSSE uses the second order Euler scheme to perform numerical integration. From the experience of these transient stability package developers, it is indicated that numerical instability problems will be avoided and the accuracy will be sufficient if the time step is kept 1/4 to 1/5 times smaller than the shortest time constant being used in the simulation.

In the validation run, PowerWorld also detected some time constants that were less than four times the time step Δt. These were reported as validation errors. The auto-correction converts these time constants to higher values to meet the criteria with reference to the time step size.

2.5 Correction of Dynamic Model Parameters

Besides machine model parameters, data errors were also found in the parameters of a particular governor model namely the 1981 IEEE type 1 turbine-governor model or commonly known as IEEEG1.

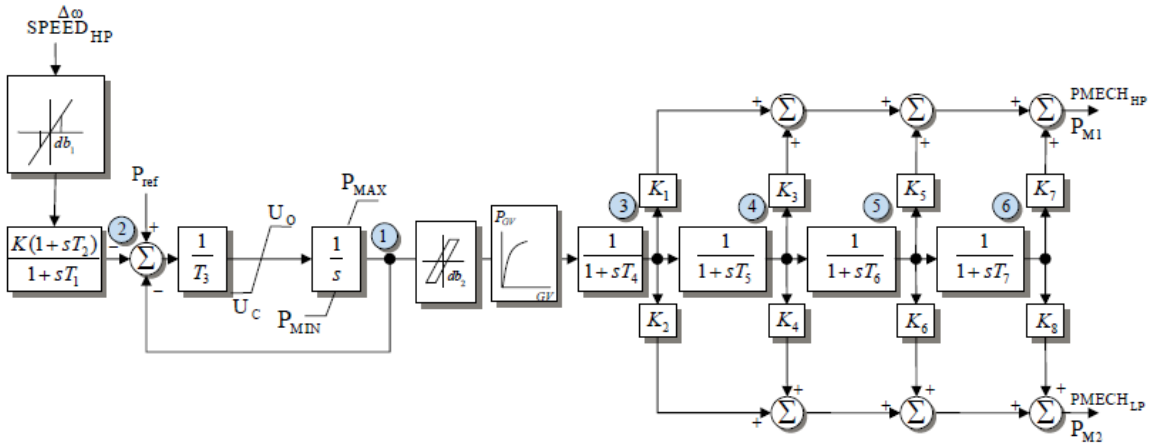

Figure 2.2: Block diagram of IEEEG1 as represented in [7]

Referring to Figure 2.2, the output of the integrator block is the total per unit mechanical power. This output gets multiplied by ($K_1+K_2+K_3+K_4$), which was found to be 20.216 in four particular governors. This sets an unreasonably high upper limit on the mechanical power output of the generator. Therefore, *($K_1+K_2+K_3+K_4$)* should be less than or equal to 1. The governor outputs have an impact on the frequency response of the system.

These validation warnings and errors thus enabled us to suggest significant changes and improvements to the dynamics data of the WECC system, which is one of the important benefits of this work.

3. Validation and Debugging Process: Top-Down Approach

This chapter highlights how large case simulations were used to detect potential analysis software problems. This example uses WECC Case 4. The validation process was comparing the transient stability runs done in PowerWorld Simulator Version 16 (beta) with the PSLF Dynamics Susbsystem (PSDS) Version 17 results provided by BPA. During the simulation the bus frequencies and voltages were monitored at 20 locations selected by BPA to give a representation of system behavior. For the simulations, the system was initially allowed to run unperturbed for two seconds to demonstrate a stable initial contingency. Then at time t = 2.0 seconds, 2 large generating units in the southern part of the WECC system were dropped and the simulation was run for a total of 30 seconds. In PowerWorld the simulation was run using a ½ cycle time step. Figures 3.1 and 3.2 show the per unit voltage magnitudes and bus frequencies at the selected buses.

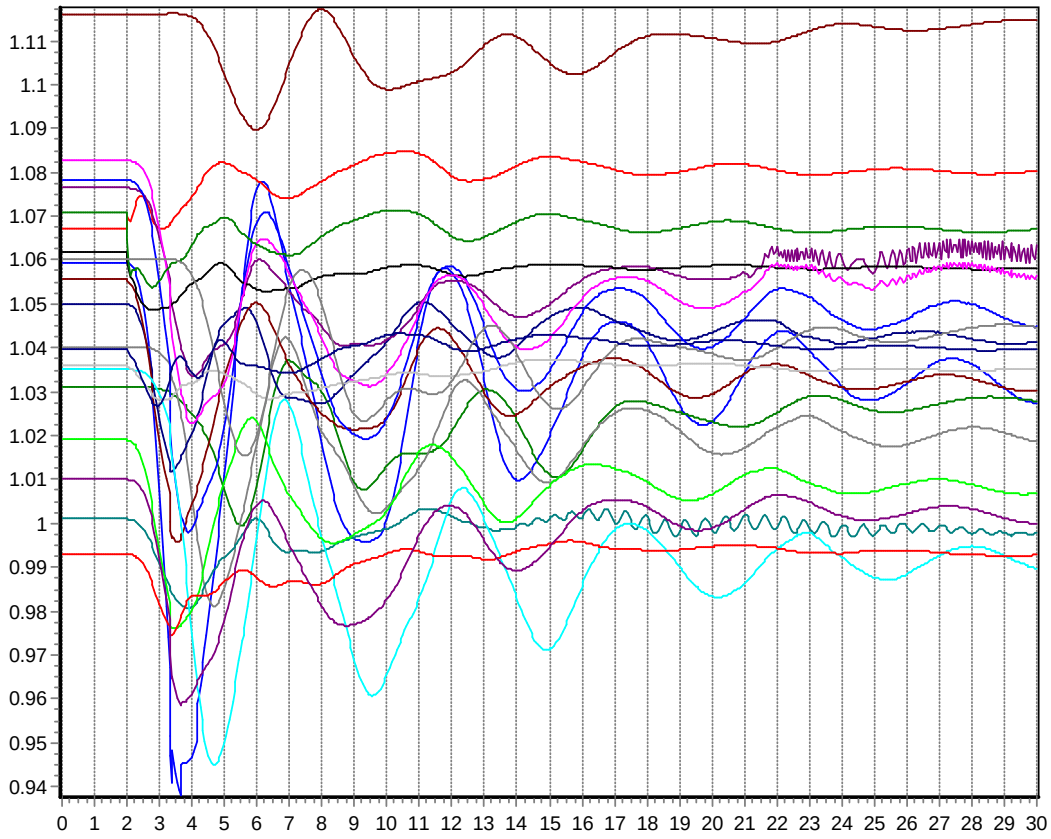

Figure 3.1: Initial per unit bus voltage magnitudes for 30 seconds of simulation in PowerWorld

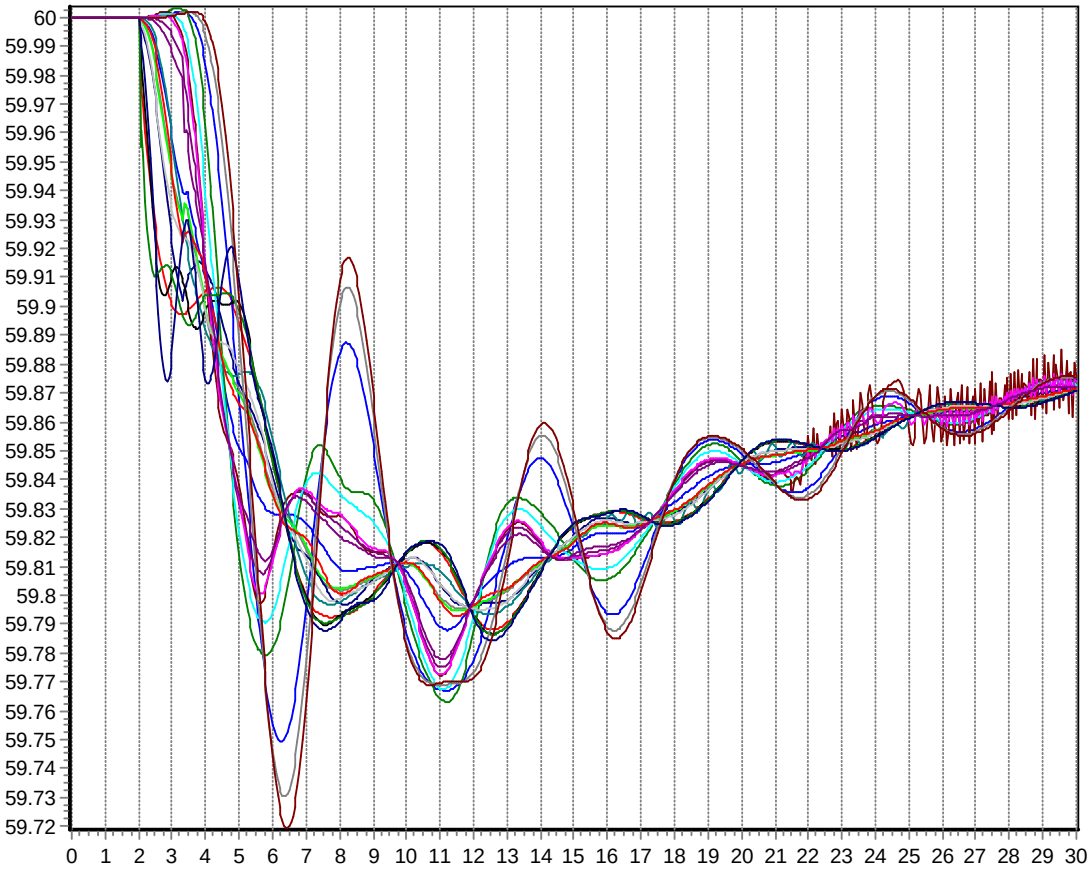

Figure 3.2: Initial bus frequencies for 30 seconds of simulation in PowerWorld

Prominently visible in Figure 3.1 is the oscillation starting at about 13 seconds into the simulation. This example details how this anomaly was used to help validate and improve the software PowerWorld. Given that this oscillation did not appear in any of the other voltage magnitude plots, it appears to be an isolated issue. Using the plotting tool's interactive features, the associated bus is immediately identified as Bus 11. However, the cause is unlikely to be at that bus.

The next step in the validation was to determine whether this oscillation also occurs in the PSLF results. Figure 3.3 compares the voltage magnitude at this bus for the two simulations. Clearly the results differ, but the most germane issue here is that the oscillation does not appear with PSLF. So the focus was to determine what is causing the

oscillation in PowerWorld. Switching from the plotting tool to the detailed results showing the voltages at all the buses, isolated plots can be quickly created.

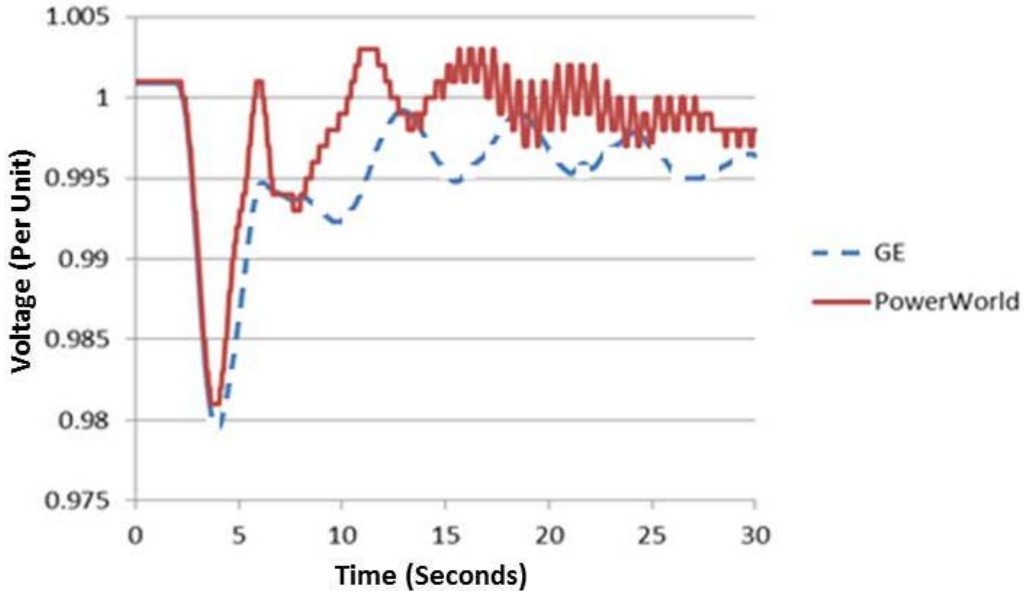

Figure 3.3: Comparison of GE-PSLF and PowerWorld results
for voltage magnitude at Bus 11

Figure 3.4 shows a plot of the voltage at Bus 11. Since this is a high voltage bus with no generation, the cause of the oscillations is not at that bus. One approach to tracking down the source of the oscillations is to look at first neighbor buses to see which have larger or smaller oscillations. This is done in the next three figures (Figures 3.5 to 3.7) for the three first neighbor buses. In this case the oscillation appears to be in the direction of Bus 12, which is joined to Bus 11 through three low impedance branches, and not in the direction of the other two branches, which have relatively higher impedances. The process is then repeated for the neighbors of Bus 11, with the highest shown in Figure 3.8 for Bus 15. Repeating one last time results in the identification of likely sources of the oscillations, two near identical generators at Buses 16 and 17 (the voltage at Bus 16 is shown in Figure 3.9).

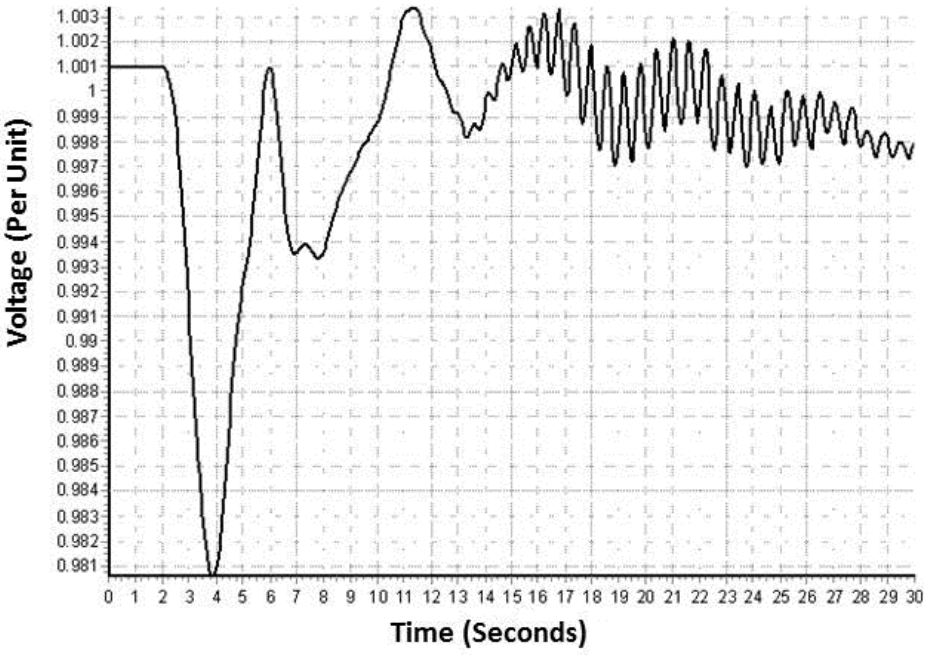

Figure 3.4: Quick plot of voltage magnitude at Bus 11

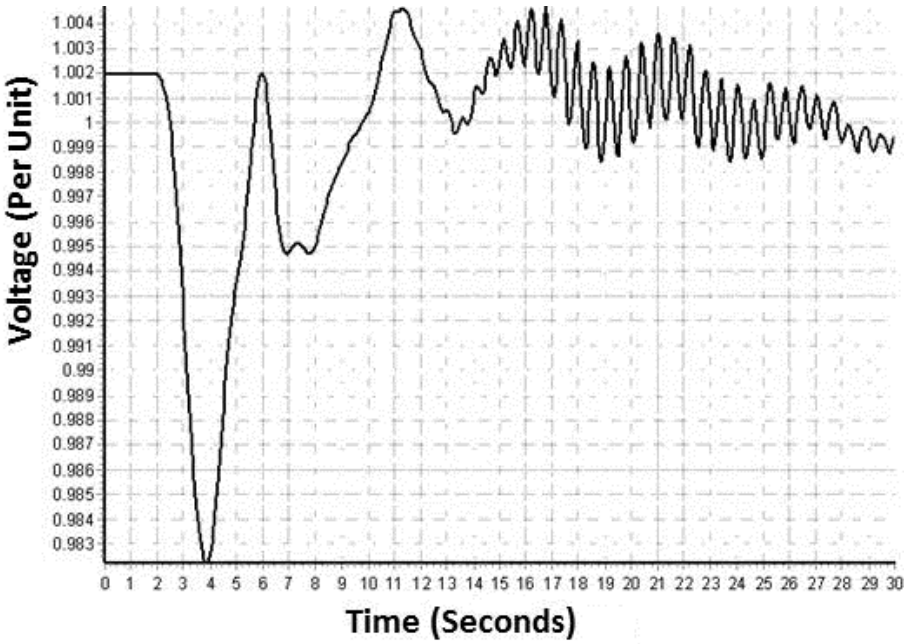

Figure 3.5: Quick plot of voltage magnitude at 1st neighbor Bus 12

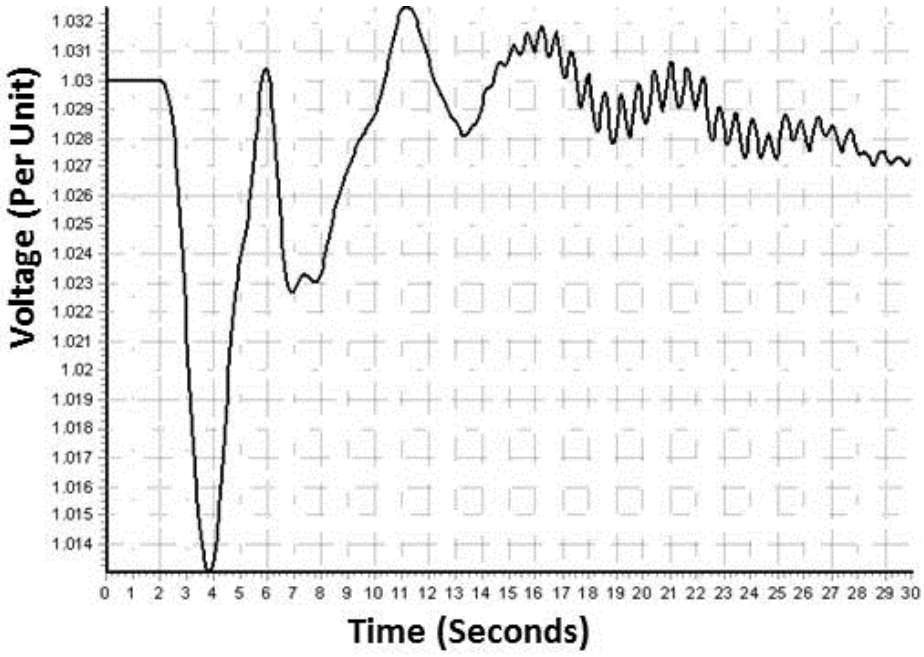

Figure 3.6: Quick plot of voltage magnitude at 1st neighbor Bus 13

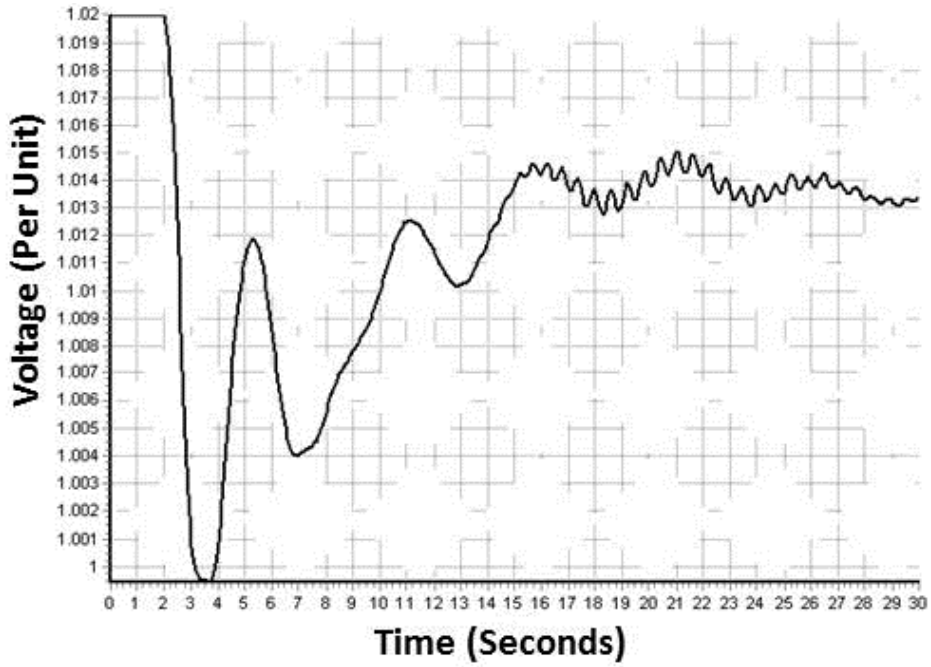

Figure 3.7: Quick plot of voltage magnitude at 1st neighbor Bus 14

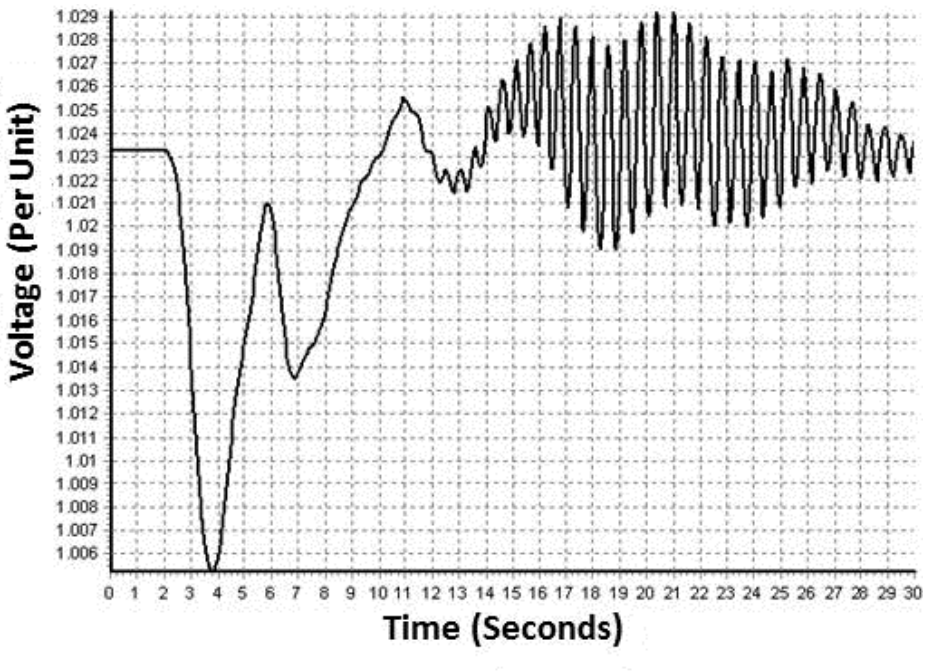

Figure 3.8: Quick plot of voltage magnitude at 2nd neighbor Bus 15

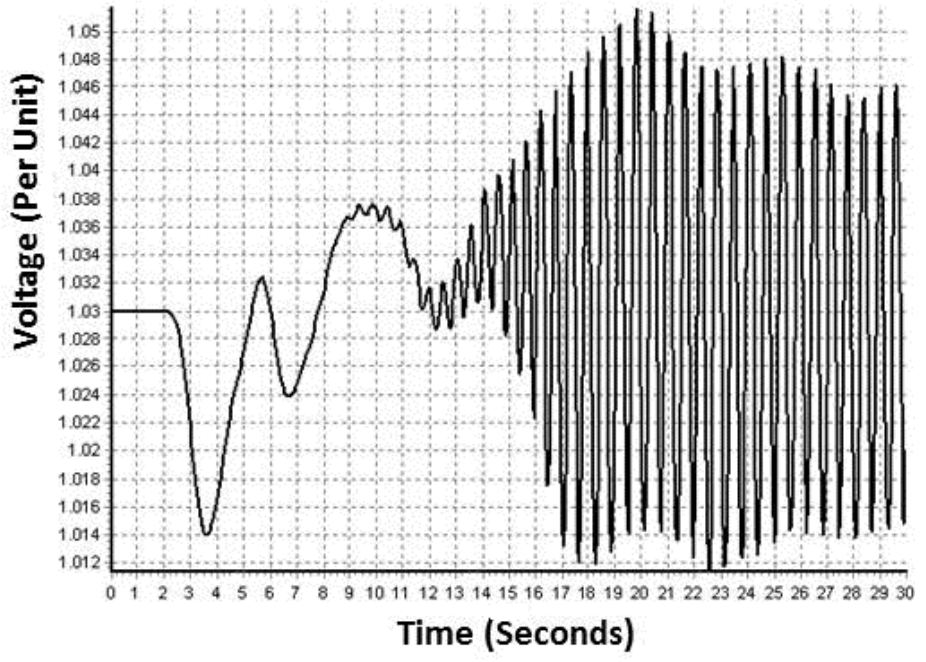

Figure 3.9: Quick plot of voltage magnitude at generator Bus 16
(note the change in Y-axis scaling from the earlier plots)

An alternative process is to utilize the SMIB eigenvalue analysis process to see if there are any generators with positive eigenvalues in the vicinity of Bus 11. For this example, this process worked quite quickly since there were only two generators in the same area as 11 with positive eigenvalues, 16 and 17.

Regardless of the process, once the problem generator or generators have been identified, the next step is to determine the reason for the unexpected behavior. A useful approach is to create a two-bus equivalent consisting of the desired generator supplying an infinite bus through its driving point impedance. This is what we term as the single machine infinite bus equivalent. PowerWorld allows this to be done in an automated process. Once the two bus equivalent is created, a balanced three phase fault is placed on the terminals of the generator at time t=1.0 seconds for 3 cycles to perturb the system. This provides an initial assessment of the stability of the generator, and probably a confirmation of the eigenvalue results. Figure 3.10 plots the generator's field voltage for this scenario. Clearly the generator is not stable. This result also helps to validate the eigenvalue analysis since the unstable eigenvalue had a damped frequency of 1.86 Hz, very close to what is shown in the figure.

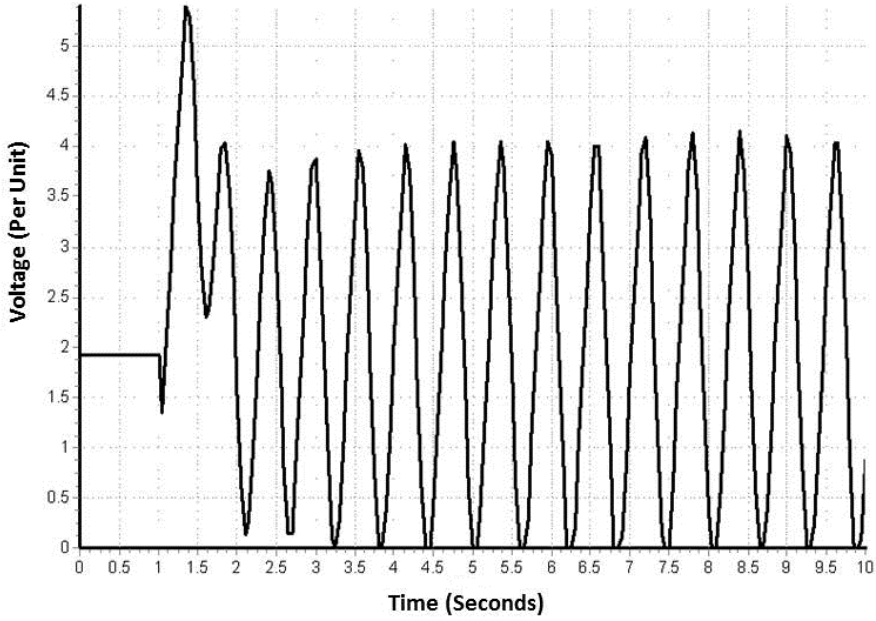

Figure 3.10: Generator 16 field voltage for two-bus equivalent fault scenario

The next step of the process is to determine whether the reason for the unstable results is an input data issue or associated with how the generator's models are represented in PowerWorld. This process is greatly facilitated by working with an SMIB equivalent, as opposed to the entire 17,000 bus WECC case. Disabling the stabilizer gives a stable result, indicating the issue is probably with the stabilizer model. Figure 3.11 shows the generator's field voltage when the stabilizer is disabled.

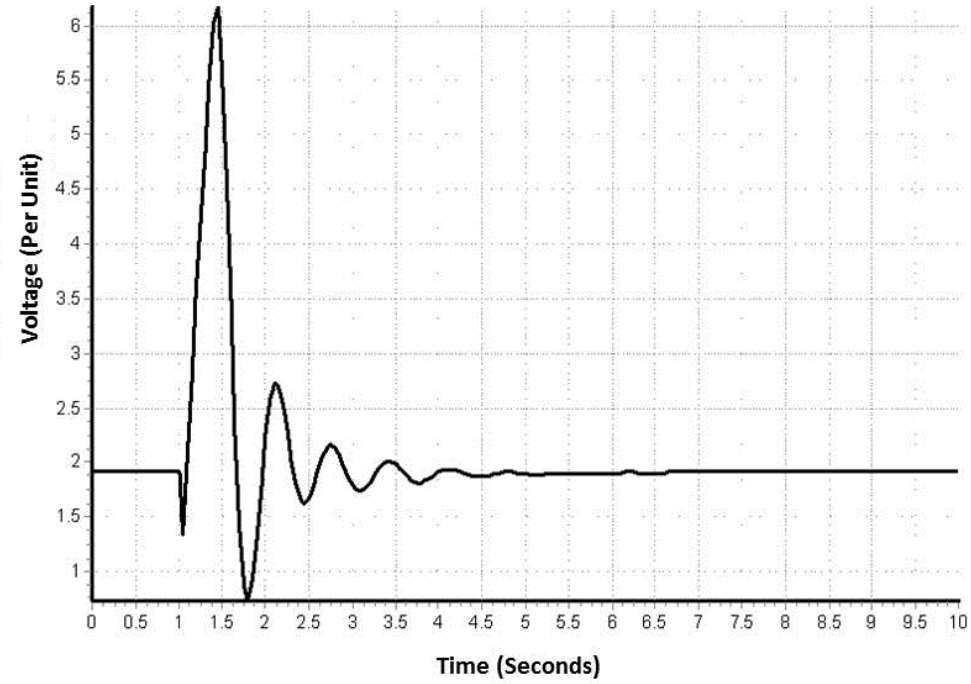

Figure 3.11: Generator 16 field voltage for two-bus equivalent fault scenario with the stabilizer disabled

Determining the exact cause of the instability is then a bit of a trial and error process, primarily through modifying parameters to see which have the most impact on the result. Another useful step is to verify that the parameters in the two-bus model actually match those in the original PSLF *.dyd file. These values might be different because of (1) an error with the input process or (2) modification by the "auto correction" during the model validation process that automatically occurs before the case is simulated.

For this example the problem was actually due to too “aggressive” auto correction of the stabilizer parameters. These generators use PSS2A stabilizer models, with the block diagram shown in Figure 3.12. For numerical stability reasons, as is common with other transient stability packages, PowerWorld was “auto-correcting” the denominator terms in the lead-lag blocks if the values were less than 4 times the time step (1/2 cycle in this case). Autocorrected values were either rounded up to 4 times the time step of 0.0333 seconds or down to zero. In comparing the values in the original *.dyd file, T_2 was being changed from 0.025 to 0.0333 while T_4 was being changed from 0.016 to 0.0 (which bypassed that lead-lag since any time the denominator in a lead-lag is zero, the numerator term must also be set to zero).

Stabilizer PSS2A

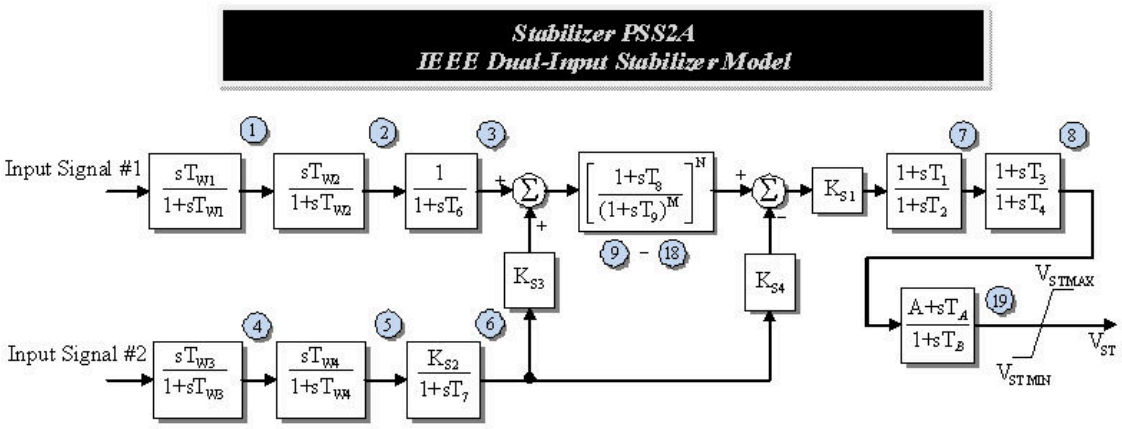

Figure 3.12: Block diagram for PSS2A stabilizer model used at generators 16 and 17

Using the SMIB equivalent, the original values were restored and tested. This gives the stable results shown in Figure 3.13. PowerWorld Corporation was notified of this issue, and as a result the validation code for all the stabilizers was modified to be less aggressive. In cases in which the lead-lag denominator time constants were small, multirate integration techniques are used. Given that the WECC case has more than 1000 stabilizers, this change actually affected 1226 separate parameter values, allowing the entered values to be retained. The results of the 30 second simulation for the full WECC Case 4 with these changes are shown in Figures 3.14 and 3.15. We notice that the oscillations at Bus 11 are now gone.

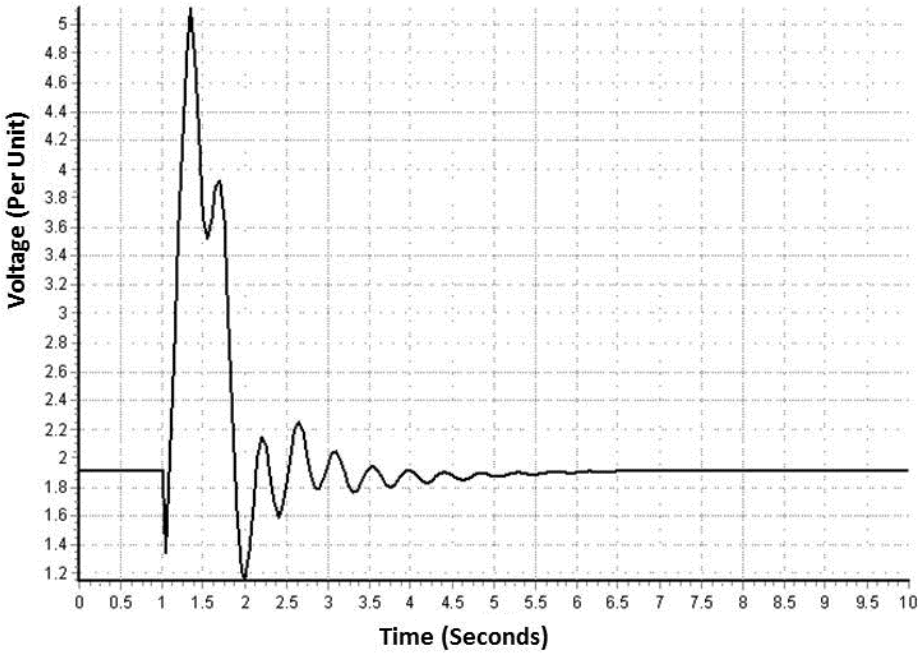

Figure 3.13: Generator 16 field voltage with stabilizer parameters returned to original value

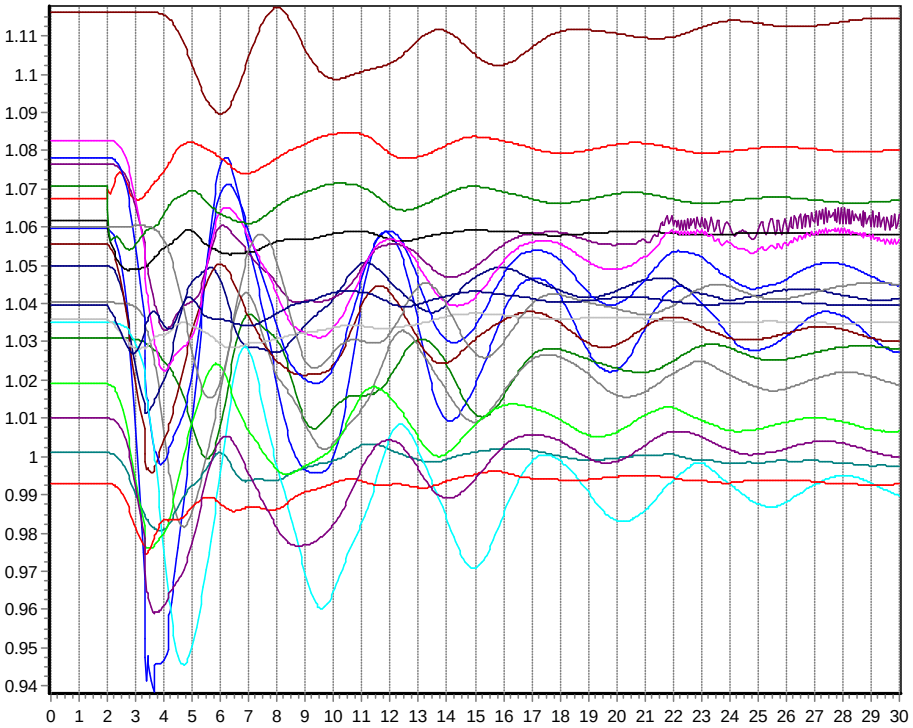

Figure 3.14: Corrected WECC case per unit bus voltage magnitudes for 30 seconds of simulation

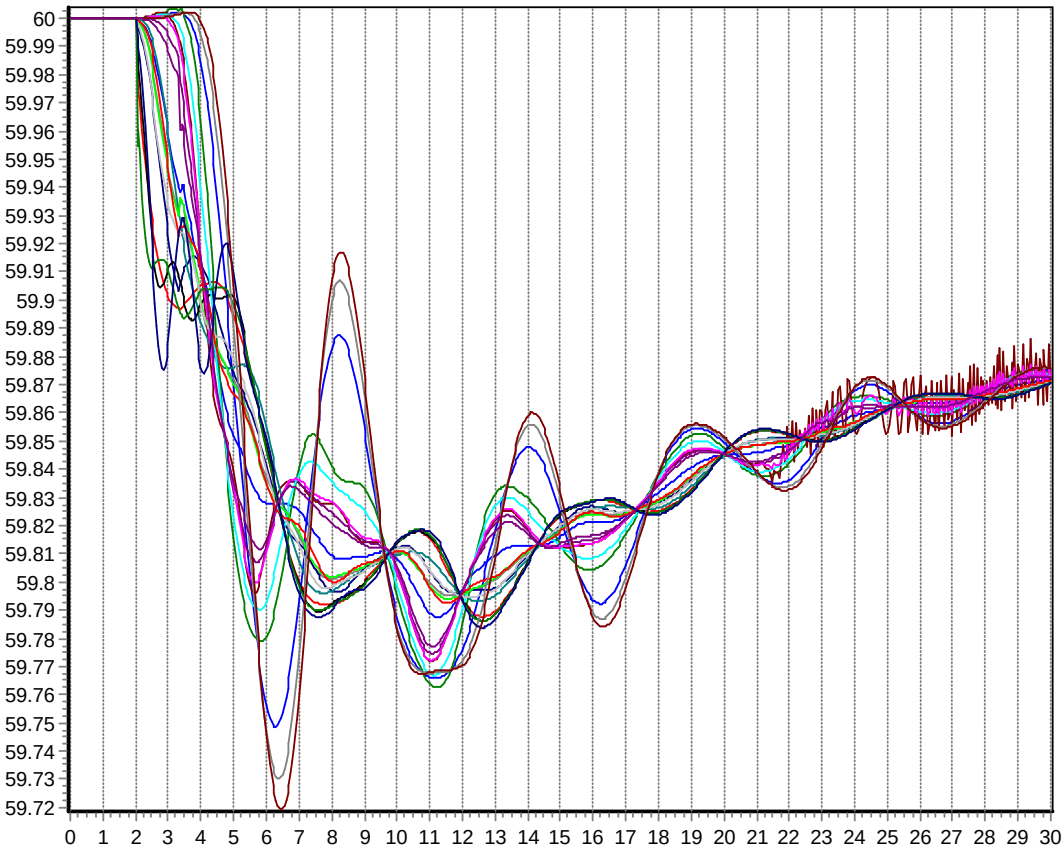

Figure 3.15: Corrected WECC case bus frequencies for 30 seconds of simulation

However, it is also readily apparent in both Figures 3.14 and 3.15 that there are some other oscillations occurring. Using a process similar to what was done previously, the bus with the most prominent oscillations was identified as being Bus 18. A comparison between the PowerWorld and PSLF results was then developed, with the comparisons for frequency and voltage shown in Figures 3.16 and 3.17. Two things are noteworthy about this plot. First, while there are certainly some differences, the overall shape of both the frequency and voltage curves is fairly similar. They start at the same values (dictated by the power flow solution), reach almost the same low values, recover at about the same rate, and return to about the same value 30 second value. Second, both packages show oscillations in the vicinity of this bus, so the issue is probably model related.

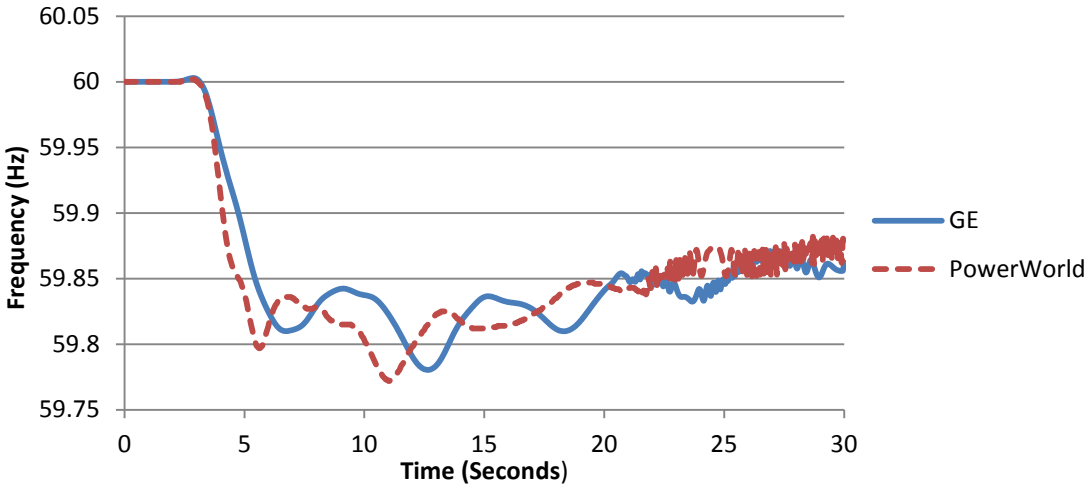

Figure 3.16: Comparison of GE-PSLF and PowerWorld results for frequency at Bus 18

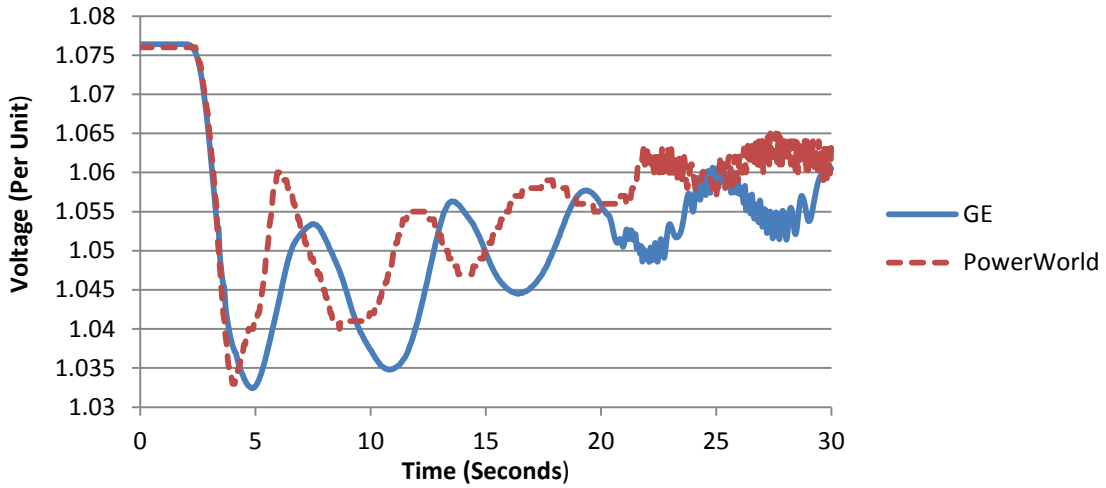

Figure 3.17: Comparison of GE-PSLF and PowerWorld results for voltage magnitude at Bus 18

In this case the "guilty" generator was identified by looking at the Bus Min/Max Voltage Summary display. For each bus in the system this display shows the highest and lowest voltage magnitudes obtained during the study for each bus in the system. Bus 19 was found to have by far the lowest voltage of 0.2404 per unit. The generator could also have been identified through eigenvalue analysis (it has a positive eigenvalue), or by tracing the magnitude of the oscillations (more tedious though since it is seven buses away from Bus 18). Figure 3.18 shows a plot of the Bus 19 voltage magnitude.

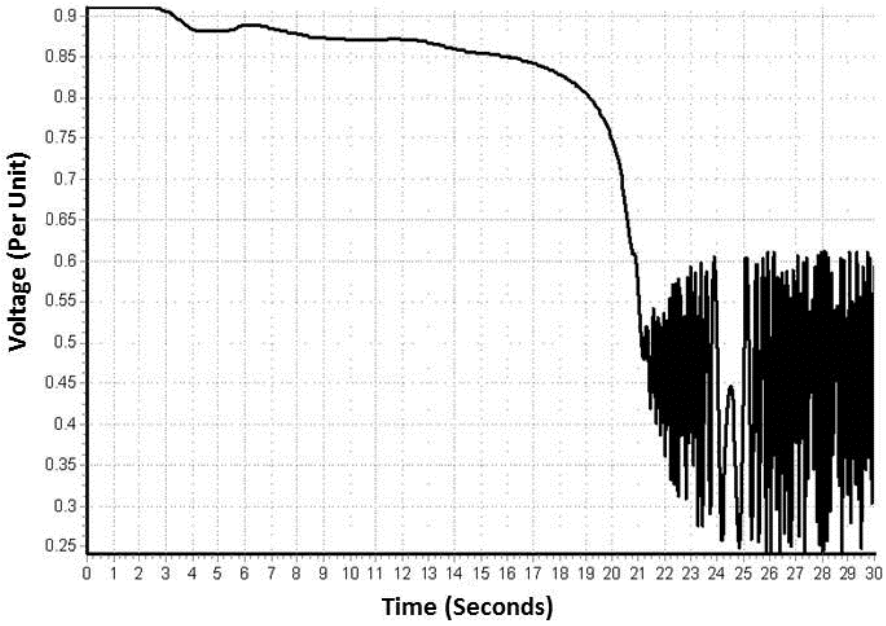

Figure 3.18: Bus 19 voltage magnitude results in PowerWorld

By again creating a two-bus equivalent, tracking down the reason for the voltage oscillations was straightforward. Bus 19 is modeled with a GENTPF machine model (a two-axis generator model that allows for subtransient saliency) but without an exciter model; it also had a GGOV1 (GE General Governor/Turbine) model. In the two-bus equivalent this generator is unstable with or without the GGOV1 model. The reason is that in the power flow the generator's setpoint voltage of 1.0 per unit (for a remote bus) was quite low, causing it to operate at its lower reactive power limit of -20 Mvars. The generator becomes stable when its reactive power output is increased to about -15 Mvars. This was confirmed by re-running the WECC Case 4 with the Bus 19 voltage setpoint increased from 1.0 to 1.02 per unit (which corresponds to a generator output of -4.4 Mvar), with the voltage results shown in Figure 3.19. Note that, in the WECC Case 2 that was tested, the Bus 19 voltage setpoint was 1.03 per unit.

From the point of view of validation, we note that both PSLF and PowerWorld appeared to correctly model the Bus 19 generator instability. One really cannot expect accuracy for such an unusual operating condition in which the voltages are below 0.5 per

unit. The issue with this generator was actually first detected in PowerWorld by looking at the event log following a simulation. By default PowerWorld trips generators if their frequencies exceed a frequency threshold (by default either above 62.4 Hz or below 57.6 Hz for two seconds). This generic protection was disabled since there did not appear to be any default protection in the GE run.

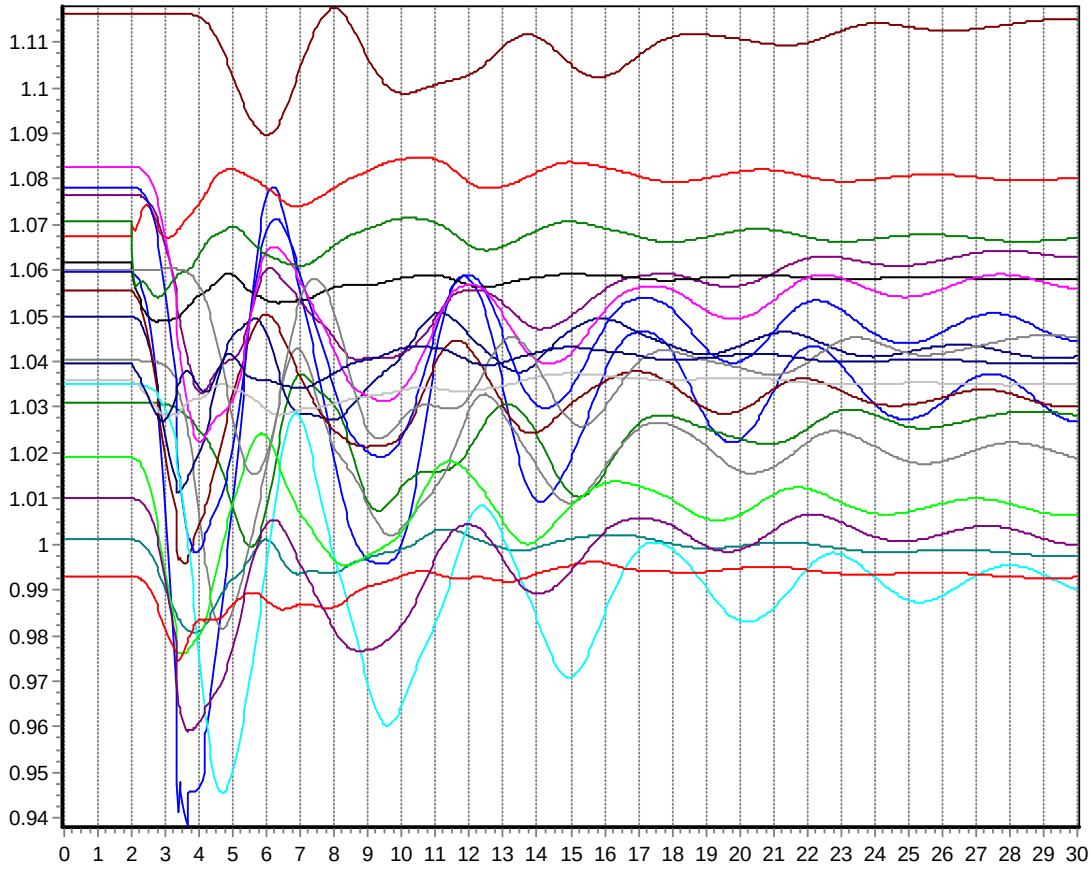

Figure 3.19: WECC bus voltages with generator voltage setpoint modified at Bus 19

Thus, this example highlights the significance of tracking down the cause of discrepancies between results obtained for the full 17,000 bus case from different packages by analyzing SMIB equivalents to focus on individual dynamic models associated with generators.

4. Validation Using Single Machine Infinite Bus Equivalents / Bottom-Up Approach

4.1 Background

This chapter describes the second methodology of validation that we developed. Here we focus on analyzing the individual dynamic models to determine the source of discrepancies in the transient stability results from different softwares. Figure 4.1 gives the general structure of a power system model and its associated controls.

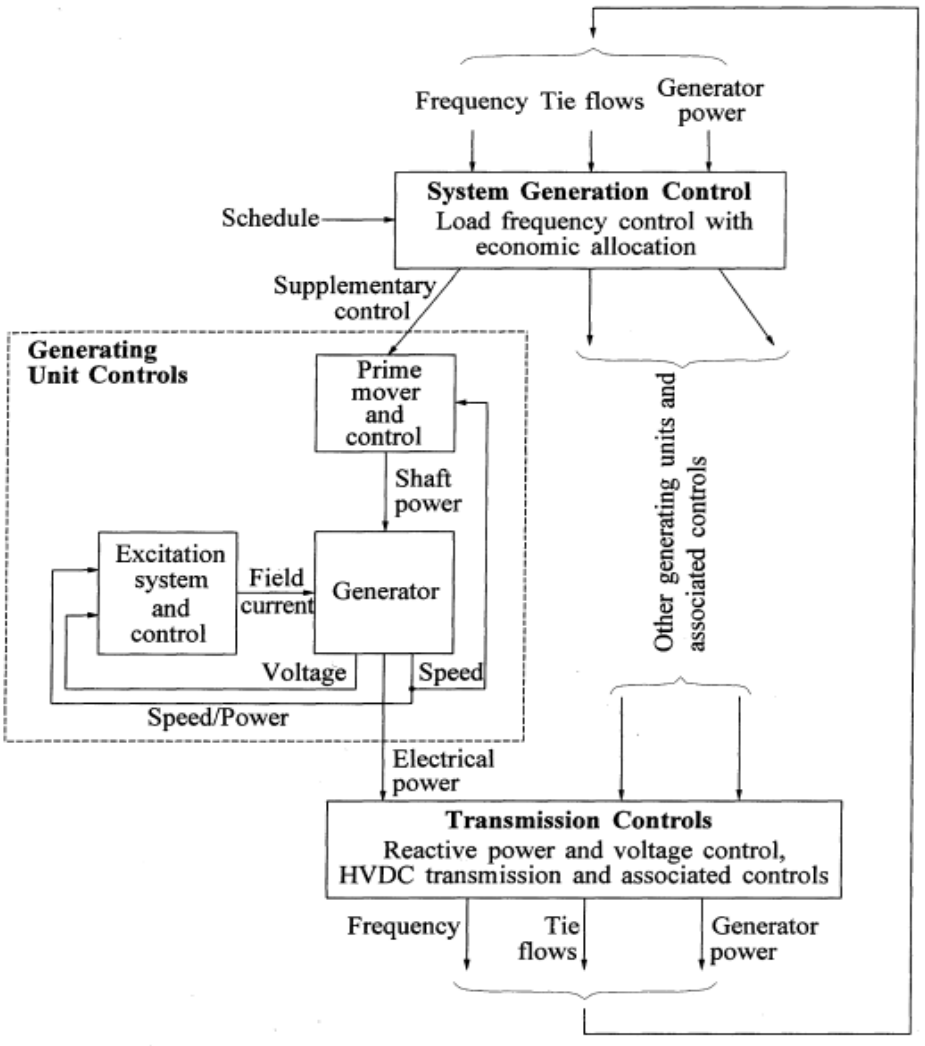

Figure 4.1: Structure of a power system model and its associated controls as depicted in [1]

We focus on the generating unit subsystem. The various dynamic models associated with a generating unit are listed below.

- Synchronous Machine Model: This is the most fundamental model used to represent the dynamics associated with a generator. It models the equations of motion of the generator, the rotor circuit dynamic equations and stator voltage equations.

- Excitation System: This system supplies direct current to the synchronous machine field winding. Additionally, by controlling the field voltage, it controls the voltage and reactive power flow. This system also performs critical protective functions like ensuring that the capability limits of the synchronous machine and other equipment are not violated. The basic elements of an excitation system include the Exciter, the Voltage Regulator, Limiters and Protective Devices and the Power System Stabilizer. In this chapter, we analyze some exciters in detail as well as a particular stabilizer model used commonly in the WECC system.

- Prime Mover and Governor: The prime movers convert raw sources of energy such as hydro and thermal energy into mechanical energy that is supplied to the synchronous generators to produce electrical energy. The governor essentially controls the power and frequency. In the subsequent chapters, we analyze certain governor models existing in the WECC system.

Apart from these two types of models, a generator model may be associated with other models like Turbine Load Controllers, Compensators, Over Excitation Limiters, etc. Certain loads such as motors are also represented by particular dynamic models. The focus of this work, though, is purely on the generation side.

The full WECC case has a total of 17,709 dynamic models in 77 model types. But the 20 most common model types contain 15,949 (90%) of these models. These are the key focus areas for the bottom-up analysis, which is discussed in the following sections.

The approach can be briefly described as follows. First, we validated SMIB equivalents consisting of only the machine model, to isolate it from any other potential source of error. Then, to the validated machine models, we add elements such as an

exciter or a governor. Any discrepancies found in the SMIB results can then be attributed to that particular model. Once the exciter has been validated, we can add a stabilizer to correctly analyze it. Thus we can go on adding models to the machine model in an SMIB equivalent one at a time and validate a new type of model at each step. This methodology forms the crux of the bottom-up approach.

4.2 Machine Model Validation

In WECC Case 4, there are a total of 3308 machine models in the whole system. The Round Rotor Generator Model with Quadratic Saturation (GENROU) and the Salient Pole Generator Model with Quadratic Saturation on d-Axis (GENSAL) account for two-thirds of these 3308 machine models. Hence validating these key models will certainly have a big impact in providing validation of the generators in the WECC system.

4.2.1 GENROU – Round Rotor Generator Model with Quadratic Saturation

Figure 4.2 shows the comparison between PowerWorld and PSSE results on a single machine infinite bus equivalent case obtained from WECC Case 1, at Bus 20, generator (Gen) 1. A solid three-phase balanced fault was applied at t = 1 sec at this bus, which was self-cleared in 0.05 sec. Thereafter the response is shown for 10 seconds. A time step of ½ cycle was used.

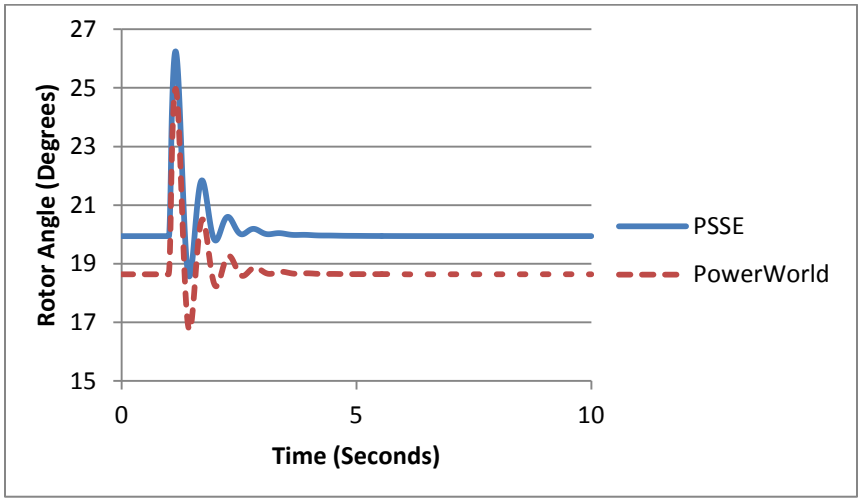

Figure 4.2: Comparisons between rotor angles for SMIB equivalent at Gen 1, Bus 20

The rotor angle comparison clearly points to an issue in the initialization process. To get to the root of this, we explored another more publicly available example referring to Figure 4.3, obtained from [8] used for basic dynamic simulation studies.

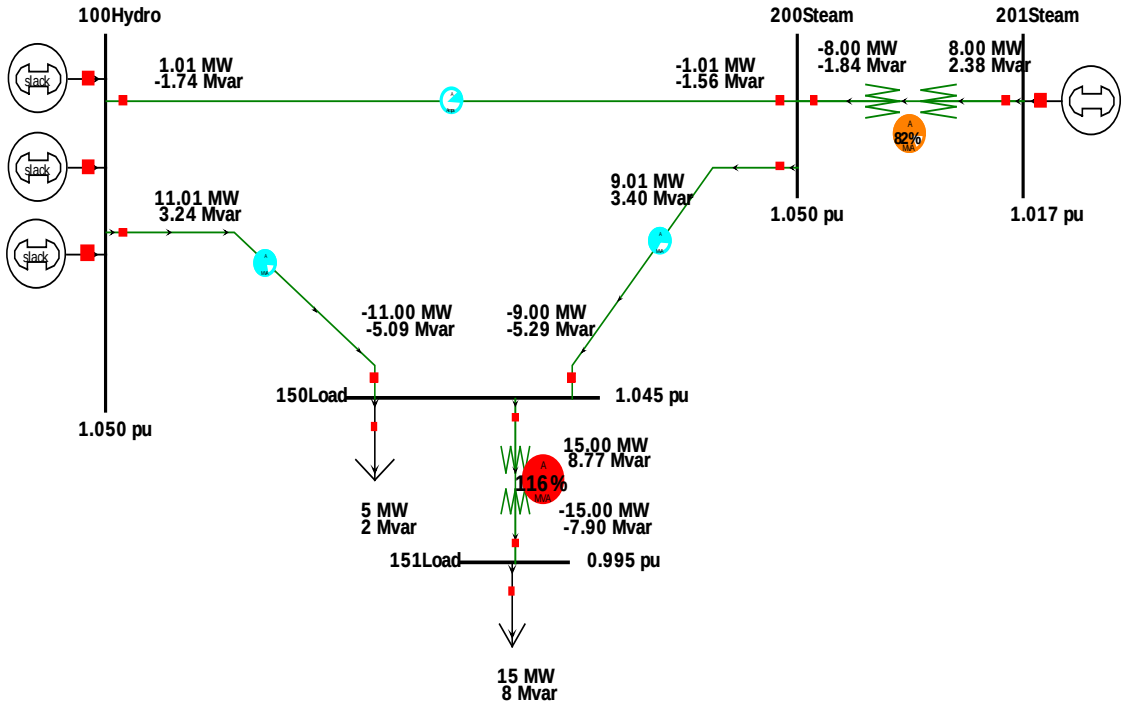

Figure 4.3: Five-bus example system

The generator at Bus 201 Steam has a GENROU model for the purpose of our study. We compared the initialization of states for the GENROU model in PowerWorld and PSSE and the following results were obtained. Initialization is more challenging when saturation is included in the machine model, so we studied the system for different values of saturation. The results are shown for a fixed value of S(1.0) = 0.03 with increasing values of S(1.2). Table 4.1 represents the PSSE results and Table 4.2 gives PowerWorld results.

Table 4.1: Initialization of GENROU model states at bus 201 Steam of the 5 bus case in PSSE for different saturation levels

S(1.2) →	**S(1.2) = 0.4**	**S(1.2) = 1.0**	**S(1.2) = 2.0**
STATES ↓			
Eqp	1.014	1.028	1.045
Edp	0.3086	0.2704	0.2195
PsiDp	0.8830	0.9000	0.9212
PsiQpp	0.5553	0.5273	0.4894
Δspeed (p.u.)	0	0	0
Angle (radians)	0.6980	0.666	0.6250

Table 4.2: Initialization of GENROU model states at bus 201 Steam of the 5 bus case in PowerWorld for different saturation levels

S(1.2) →	**S(1.2) = 0.4**	**S(1.2) = 1.0**	**S(1.2) = 2.0**
STATES ↓			
Eqp	1.0152	1.0299	1.0478
Edp	0.3061	0.2651	0.2099
PsiDp	0.8842	0.9023	0.9249
PsiQpp	0.5535	0.5234	0.4822
Δspeed (p.u.)	0	0	0
Angle (radians)	0.6959	0.6623	0.6172

This process enabled us to identify the issues in the initialization process. These discrepancies were reported to PowerWorld. The issue that was tracked down was that the non-linear (quadratic) initialization equations for GENROU to account for generator saturation were not being solved appropriately. This was corrected, the software was updated and the results were validated, as shown in Table 4.3

Table 4.3: "Corrected" initialization of GENROU model states at bus 201 Steam of the 5 bus case in PW for different saturation levels

S(1.2) →	**S(1.2) = 0.4**	**S(1.2) = 1.0**	**S(1.2) = 2.0**
STATES ↓			
Eqp	1.014	1.028	1.045
Edp	0.3086	0.2704	0.2195
PsiDp	0.883	0.900	0.9212
PsiQpp	0.5553	0.5273	0.4894
Δspeed (p.u.)	0	0	0
Angle (radians)	0.698	0.666	0.6250

The updated PowerWorld software was then used to simulate the two-bus system for Bus 20 to yield validated results as in Figure 4.4.

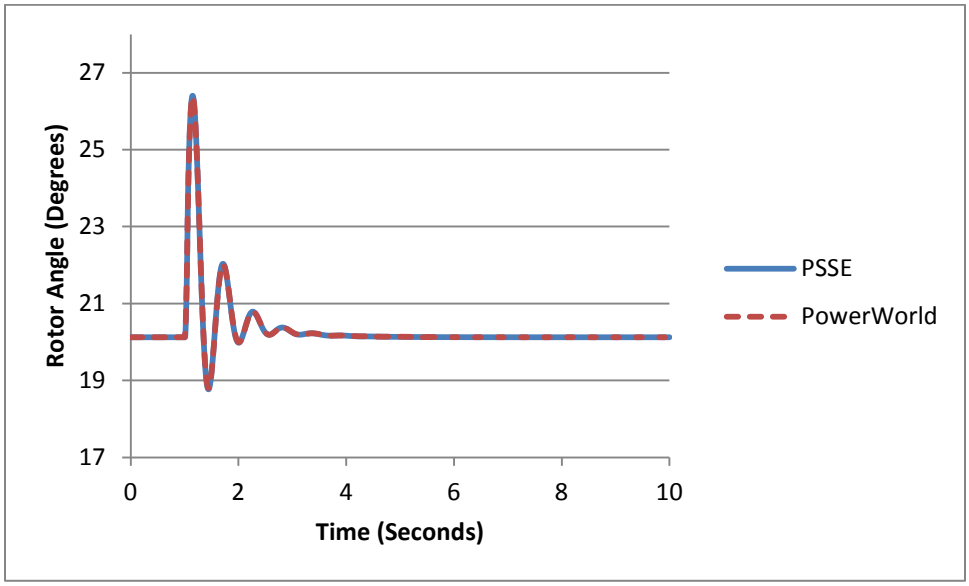

Figure 4.4: "Corrected" Comparisons between Rotor Angle
for SMIB equivalent Gen1, Bus 20

4.2.2 GENSAL – Salient Pole Generator Model with Quadratic Saturation on d-Axis

To validate this model, another two-bus equivalent was created at Bus 21, Gen 1, from WECC Case 2. In addition to the machine model, the generator here also has a Basler DECS exciter model called ESAC8B. A solid three-phase balanced fault was applied at t = 1 sec at this bus, which was self-cleared in 0.05 sec. Thereafter the response is shown for 10 seconds. A time step of ½ cycle was used. The preliminary comparisons are given in Figures 4.5 and 4.6.

Looking at these results initially, it is not trivial to figure out whether the issue lies in the machine model or the exciter or both. An important aspect of our methodology has been to break down the problem to the individual components to check for discrepancies and then add these components back until the problem is encountered again. We therefore repeated this comparison with the exciter model disabled. The results are shown in Figures 4.7 and 4.8.

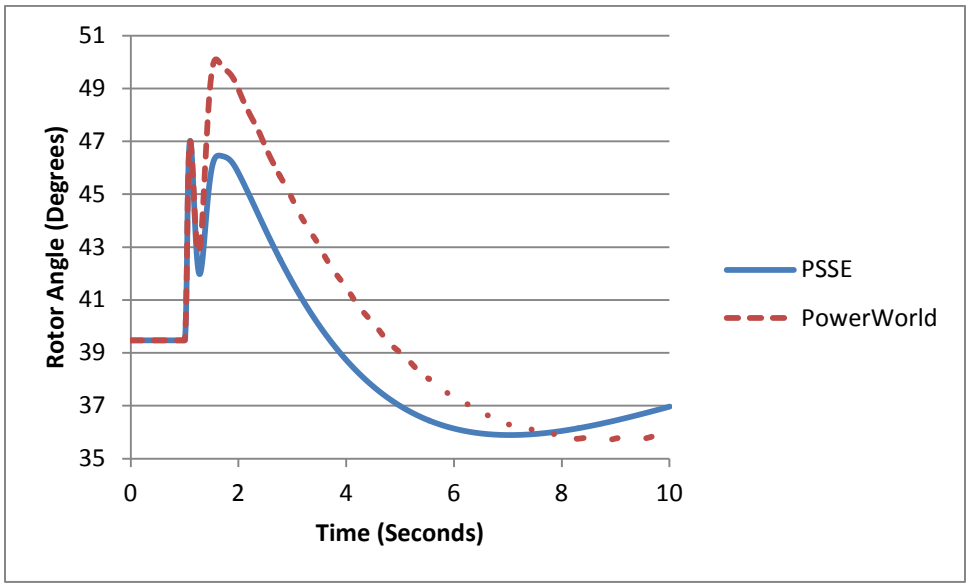

Figure 4.5: Comparison of rotor angle for the SMIB equivalent at Gen1, Bus 21

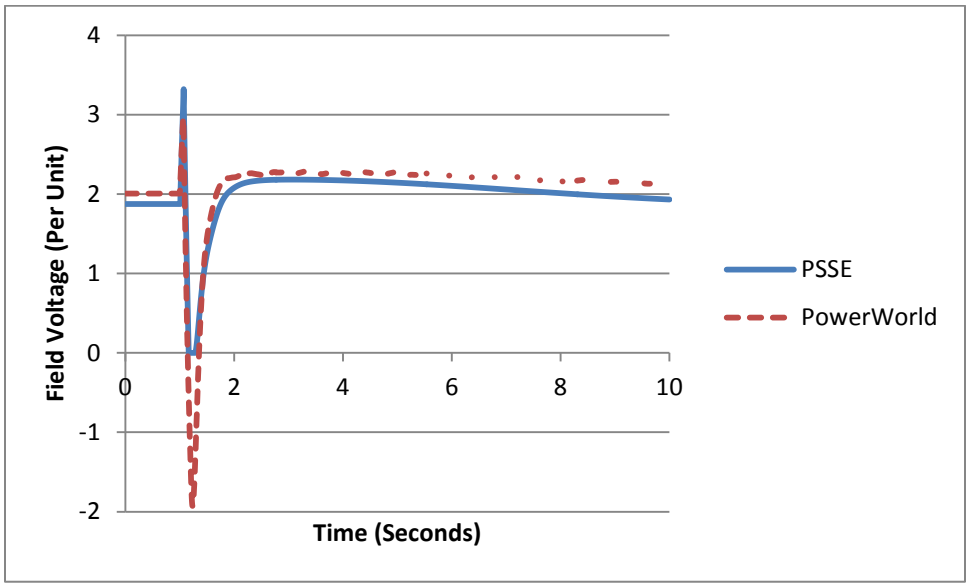

Figure 4.6: Comparison of field voltage (EFD) for the SMIB case Gen1, Bus 21

By disabling the exciter we were able to determine that there were inherent issues in the GENSAL model. From Figure 4.8, it is clear that the initialization of the field voltages is discrepant.

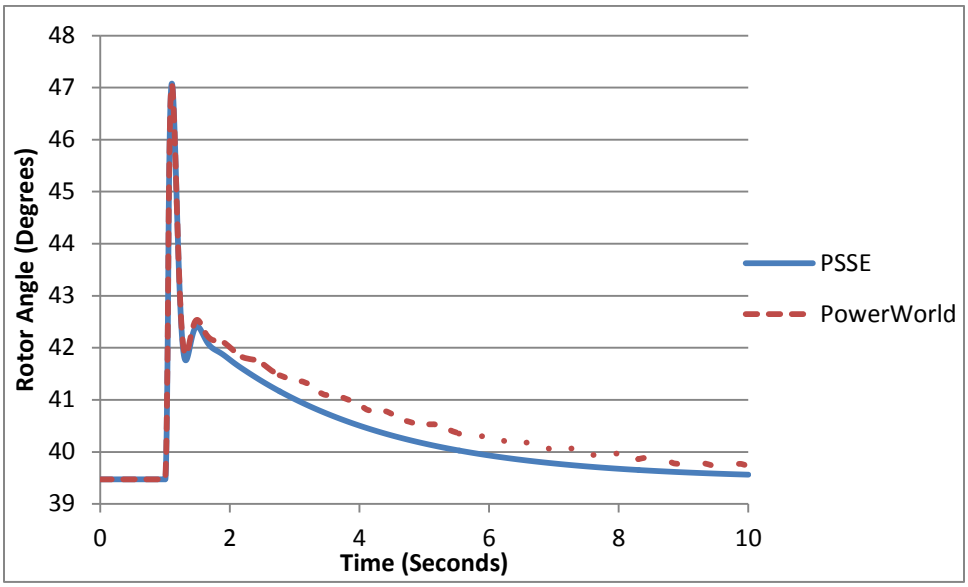

Figure 4.7: Comparison of Rotor Angle for the SMIB case Gen1, Bus 21 with the exciter disabled

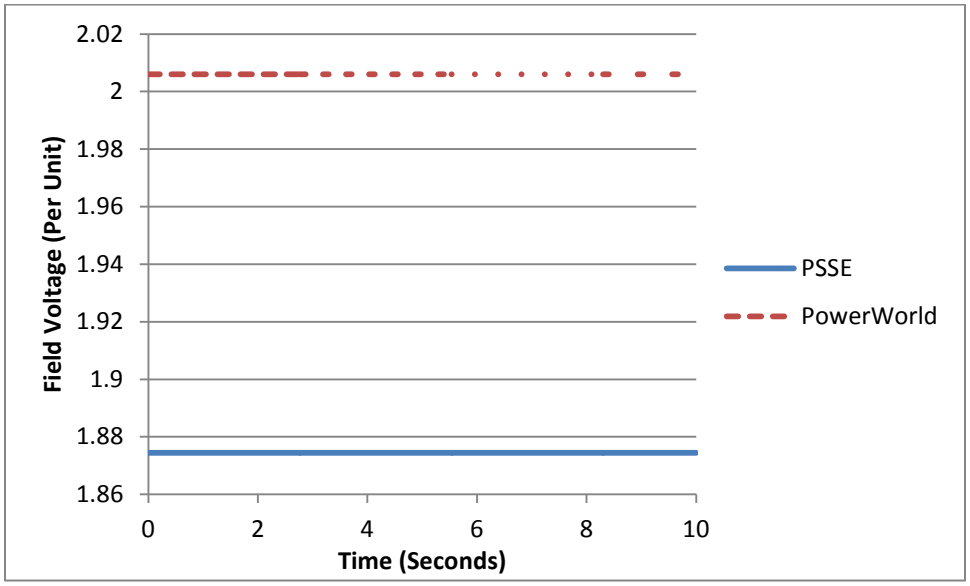

Figure 4.8: Comparison of EFD and for the SMIB case Gen1, Bus 21 with the exciter disabled

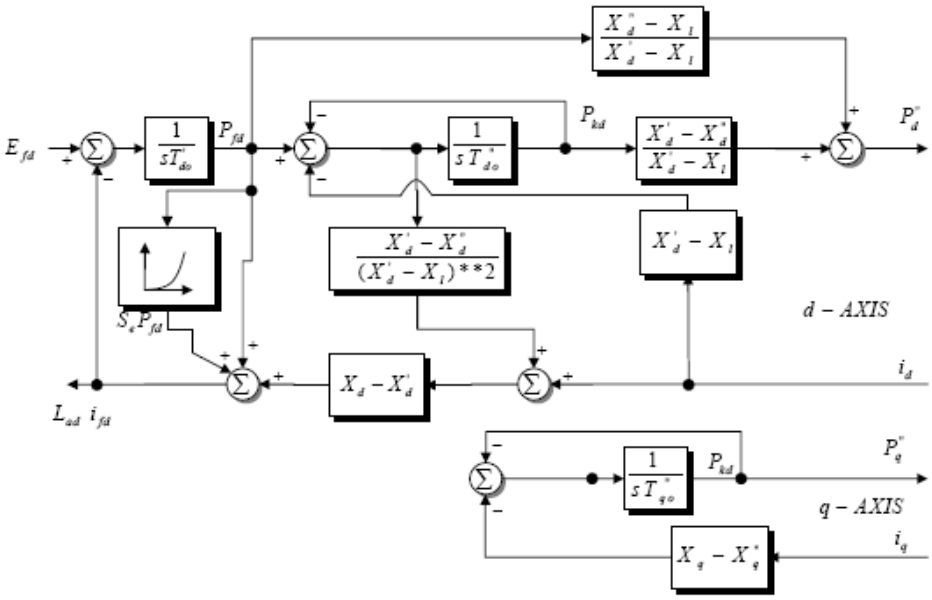

Figure 4.9: Block diagram of GENSAL model as represented in [7]

PowerWorld looked into this and found that the saturation S_e was being directly fed as an input to the field current instead of it being multiplied by the state P_{fd} as is depicted in Figure 4.9. After these corrections, the EFD initializations were now agreeing with each other, as per Figure 4.10.

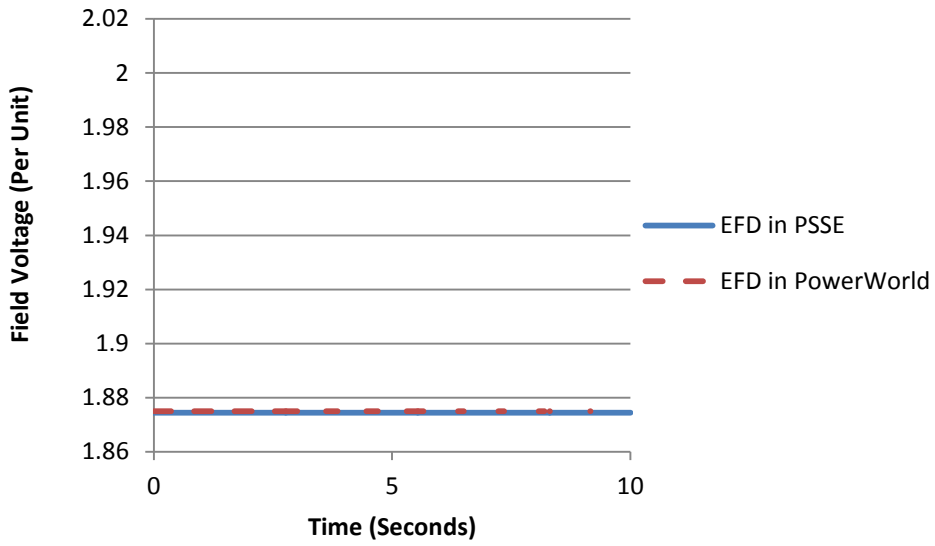

Figure 4.10: "Corrected" comparison of field voltages for the SMIB case Gen 1, Bus 21 with the exciter disabled

4.3 Exciter Model Validation

In WECC Case 4, there are a total of 2763 exciter models in the whole system. Of these, a summary of the major models, by count, is given in Table 4.4.

Table 4.4: Summary of the major exciter models in use in WECC Case 4

Name	EXST1	EXST4B	EXAC1	EXDC1	EXAC8B	REXS
Count	869	357	149	288	166	231

It is important to note here that these models are PSLF models as the base case, i.e. the full WECC case, was derived from PSLF format files (*.epc and *.dyd). There are subtle differences in the names and implementations of these models in PSLF and PSSE. Therefore to perform validation studies using PSSE, we had to convert some of these models in their PSSE "equivalent" models. For instance EXAC8B exciter model in PSLF is modeled under the name AC8B in PSSE. A WECC approved list of these equivalencies is given in [9].

4.3.1 ESAC8B – Basler DECS Model

Referring to the SMIB case Gen 1, Bus 21 discussed in the GENSAL validation process. We concluded that there were possibly some discrepancies in the exciter behavior as well.

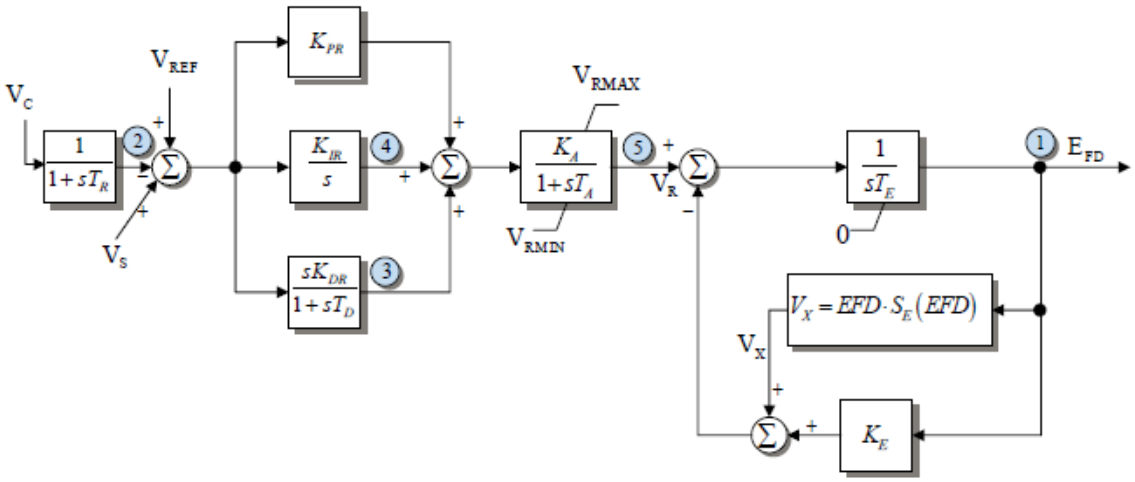

Figure 4.11: Block diagram of exciter model ESAC8B as represented in PSSE [7]

Referring to Figure 4.11, the issue was found to be due to the fact that PowerWorld was not enforcing the lower limit of 0 in the integration process to calculate EFD. Figure 4.12 shows the validation of PowerWorld results with PSSE, in a subsequent version of the PowerWorld software. As we see, the revised PowerWorld results now perfectly match the PSSE results.

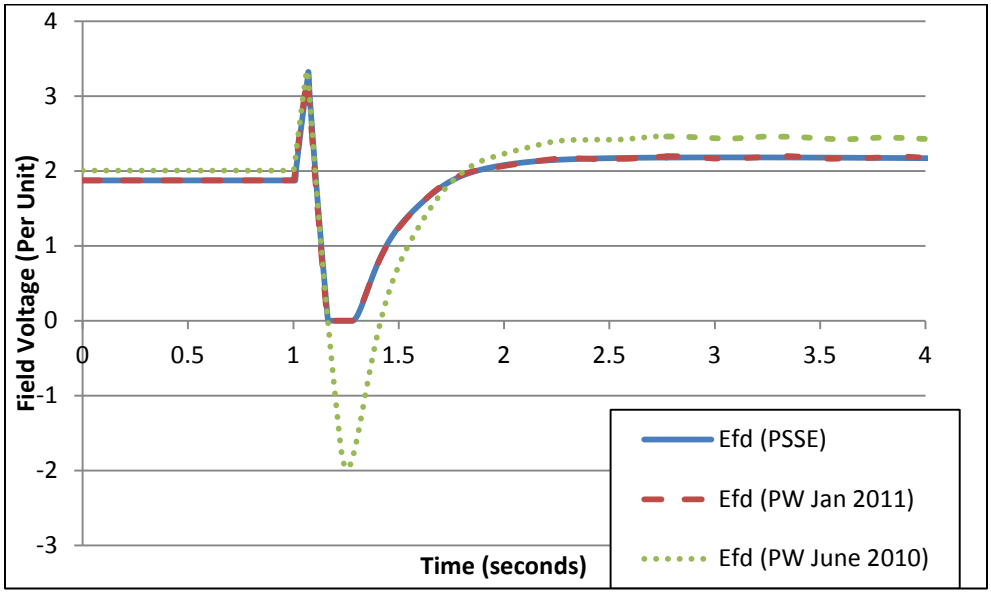

Figure 4.12: Comparison of EFD values of SMIB case at Bus 21, Gen 1 between different versions of PowerWorld and PSSE

4.3.2 Exciter Saturation Modeling

One of the most significant findings in the process of validating excitation system models was that of the existence of three different saturation functions, listed in Table 4.5, being used to model exciters.

Table 4.5: Types of saturation functions modeled in different packages for excitation systems

Type of Saturation Model	**Function**	**Software**
Quadratic	S(x) = B(x - A)^2	GE GE
Scaled Quadratic	S(x) = B(x - A)^2 / x	PTI PSS/E
Exponential	S(x) = B exp(A*x)	BPA IPF

Initially, PowerWorld was following BPA's convention of saturation modeling. However, from our benchmarking studies, we discovered two other methods that are used in PSLF and PSSE. These options have been added to PowerWorld to aid the validation process with other packages.

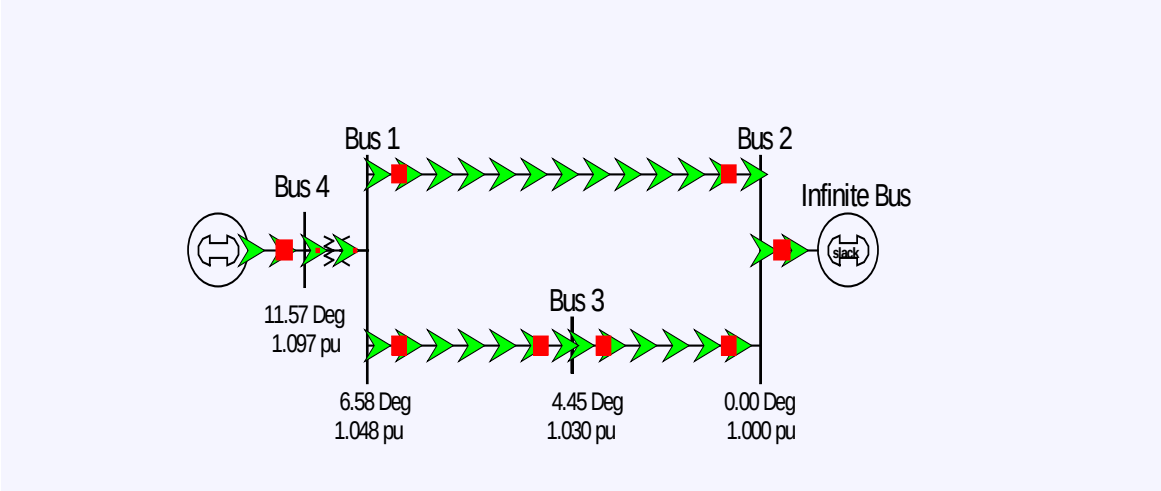

Figure 4.13: Example 4 bus case with GENROU and IEEE Type 1 Exciter (IEET1) at Bus 4

The case depicted in Figure 4.13 was used to study the impact of different types of exciter saturation modeling on the system behavior, mainly the field voltage. A solid

three-phase balanced fault was applied at t = 1 sec at Bus 4, which was self-cleared in 0.05 sec. Thereafter the response is shown for 10 seconds. A time step of 1/4 cycle was used. Figure 4.14 illustrates these differences.

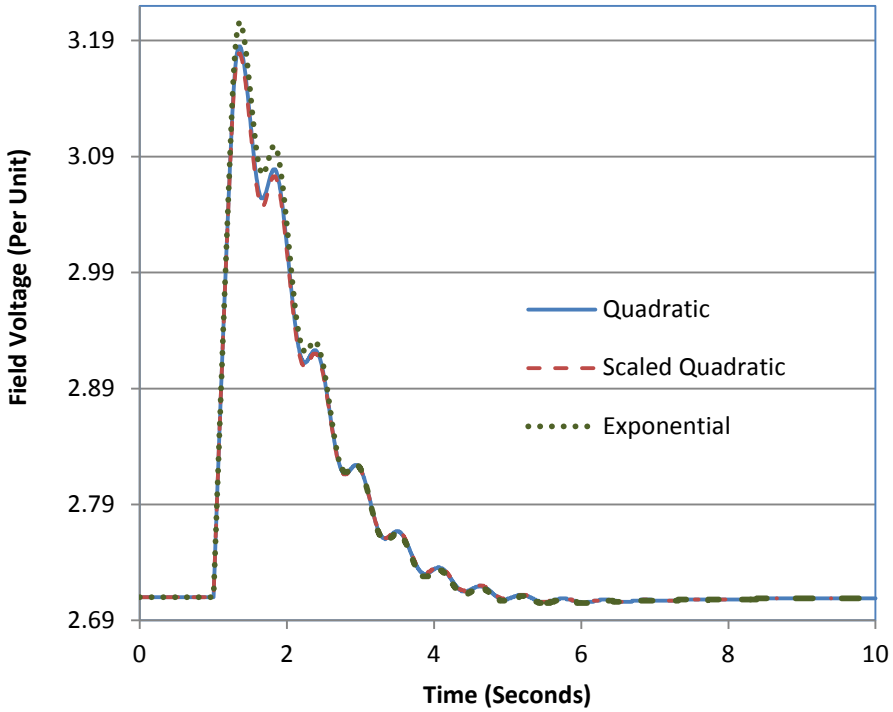

Figure 4.14: Field voltages for different exciter saturation models for the 4 bus case

4.3.3 EXAC1 – IEEE Type AC1 Excitation System

This model was validated by creating a SMIB equivalent at Bus 22, Generator 1. This generator has a GENROU machine model. The advantage of having the machine models validated before is that now the discrepancies, if any, can be attributed to the added component, i.e. the exciter. A solid three-phase balanced fault was applied at t = 1 sec at the generator bus, which was self-cleared in 0.05 sec. Thereafter the response is shown for 10 seconds. A time step of 1/4 cycle was used. Figures 4.15 and 4.16 represent the comparisons showing major discrepancies.

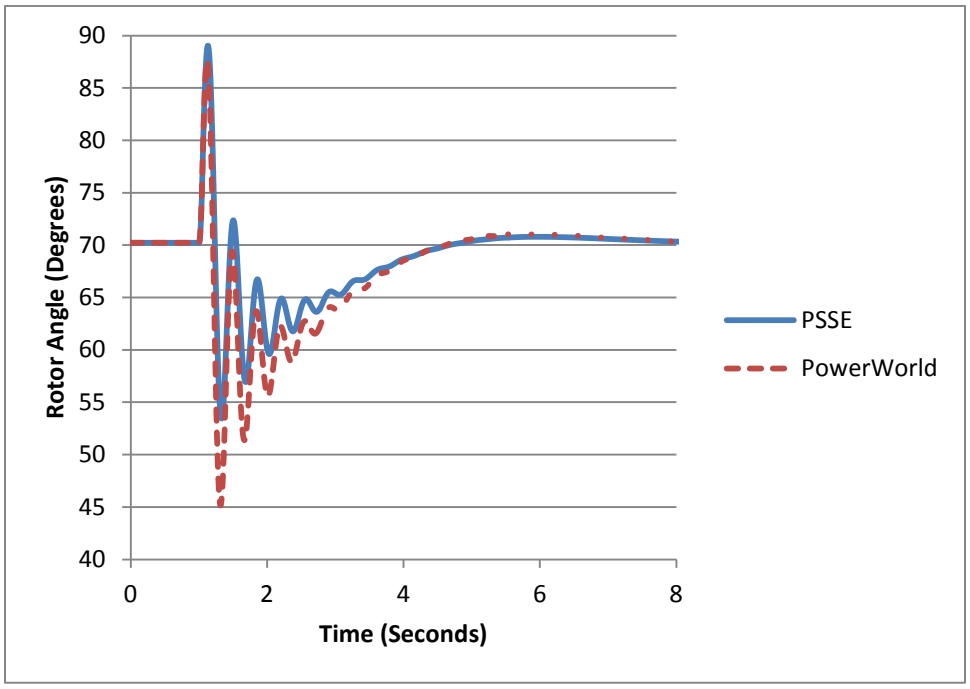

Figure 4.15: Comparison of rotor angle between PowerWorld and PSSE for SMIB case Bus 22, Gen1

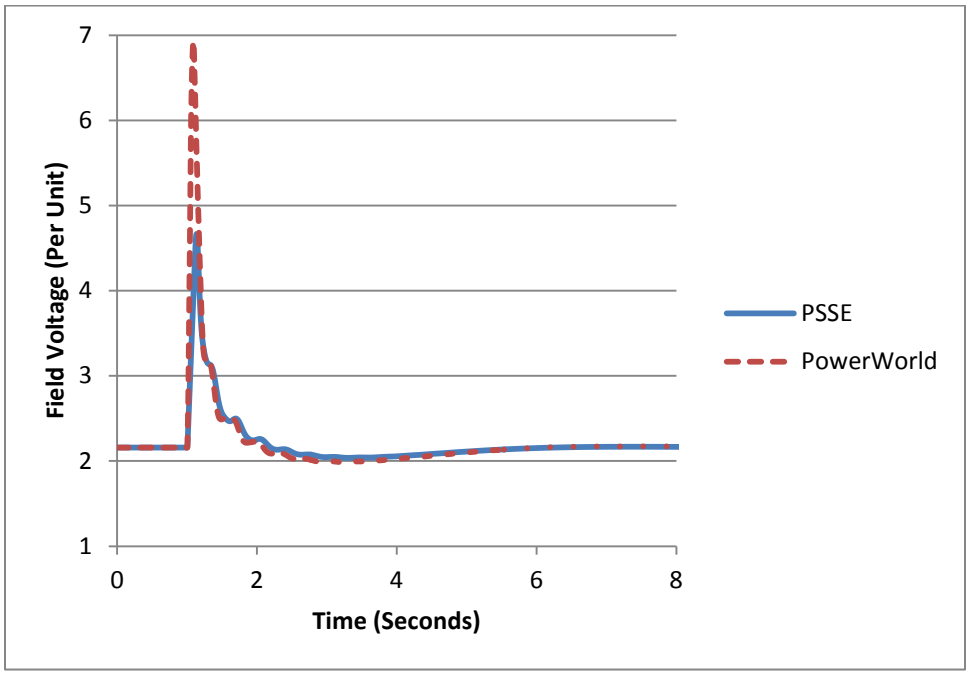

Figure 4.16: Comparison of field voltage between PowerWorld and PSSE for SMIB case Bus 22, Gen1

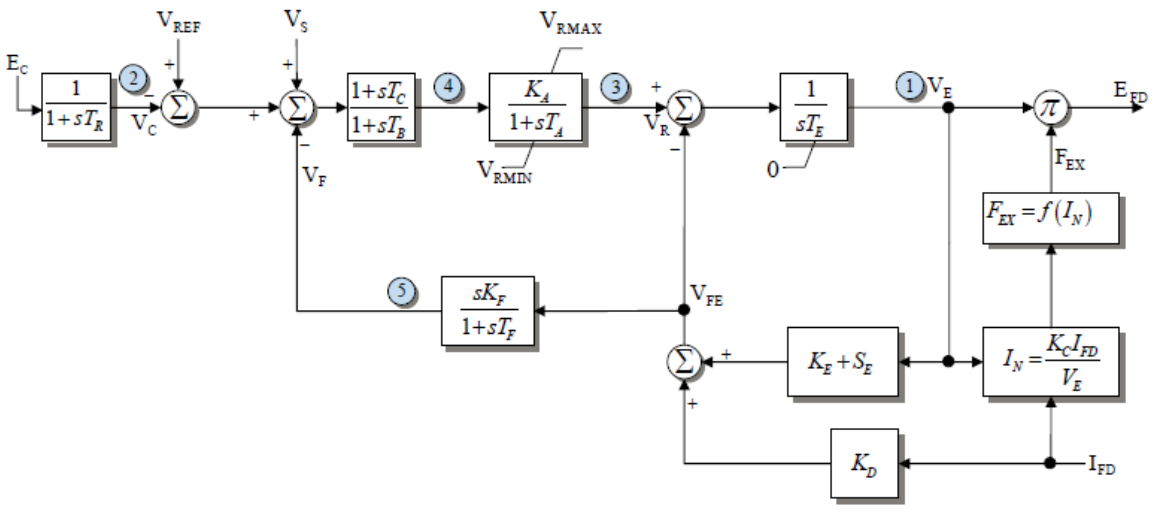

Figure 4.17: Block diagram on EXAC1 exciter in PSSE [7]

The debugging process for this case, referring to Figure 4.17, was as follows. In this SMIB case, for the exciter, the *Kc* parameter was zero. This means that *In* is always zero, meaning that *fEx* is always 1. Hence EFD is always equal to *Ve*. Since *Te* = 1 in this case, the derivative of *Ve* is just *Vr* – *Vfe*. This *Vr* has minimum and maximum limits which cap the response for *Vr*. The issue here was that *Ve* was rising too quickly in PowerWorld. We then numerically estimated the rate of change in *Ve* for the PSSE results. Since *Vrmax* = 24, the rate of change of *Ve* in PSSE, which was 20 or 21, looked correct owing to the fact that the derivative is (*Vr* – *Vfe*); *Vr* rapidly rises to its maximum during the fault and *Vfe* is a positive value. In PowerWorld, the rate of change of *Ve* was found to be much higher. This pointed to an error in the integration process for this exciter in PowerWorld. Subsequent changes were made to the PowerWorld program and this exciter was thus validated. Figures 4.18 and 4.19 show the corrected values of the rotor angle and field voltages respectively.

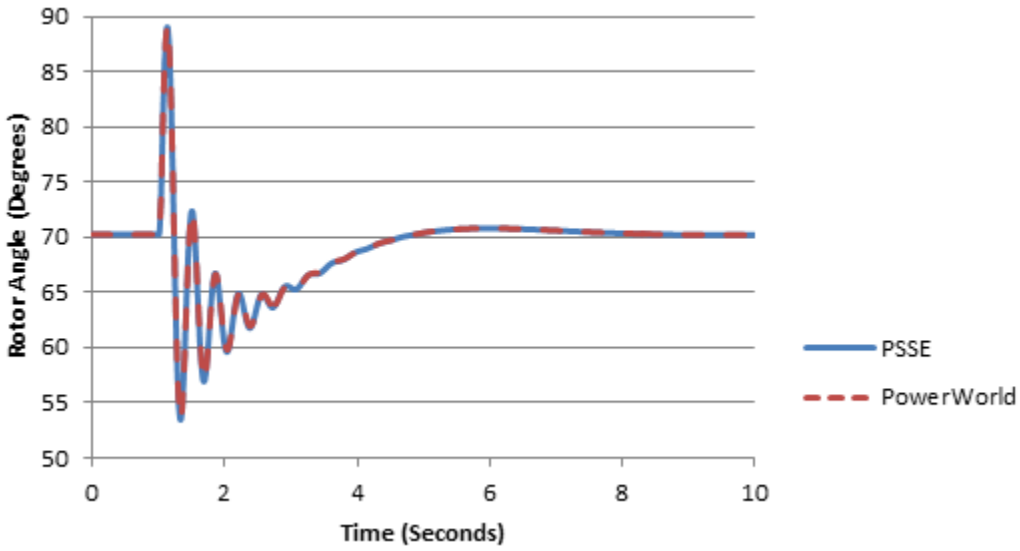

Figure 4.18: "Corrected" rotor angles for the SMIB case Gen 1, Bus 22

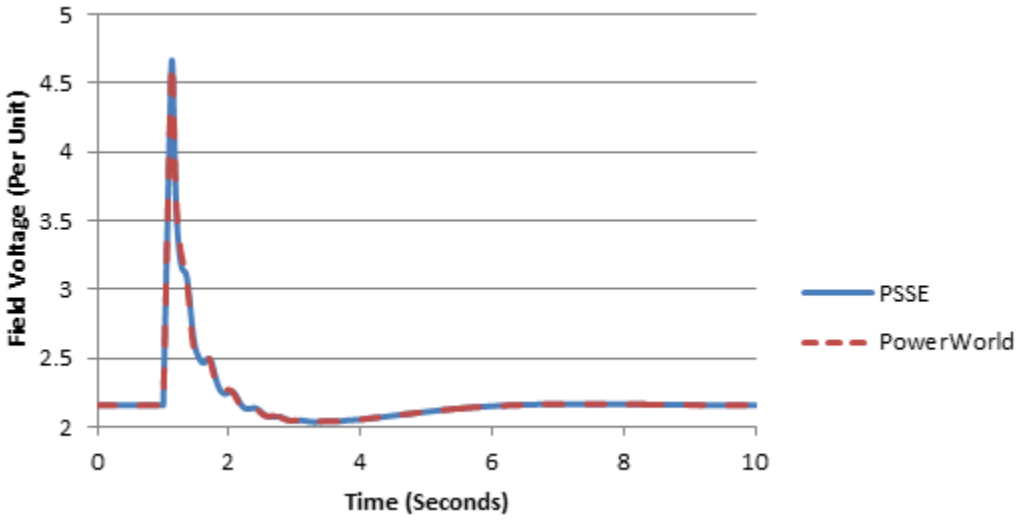

Figure 4.19: "Corrected" field voltages for the SMIB case Gen 1, Bus 22

4.3.4 EXST1 – IEEE Type ST1 Excitation System Model

This model of exciters is the most commonly used model in the WECC case. It accounts for one third of the total exciter model usage. The validation of this model was a little challenging due to its different implementations in PSLF and PSSE. PowerWorld has

implemented both these models, as EXST1_GE and EXST1_PTI, thus making validation easier.

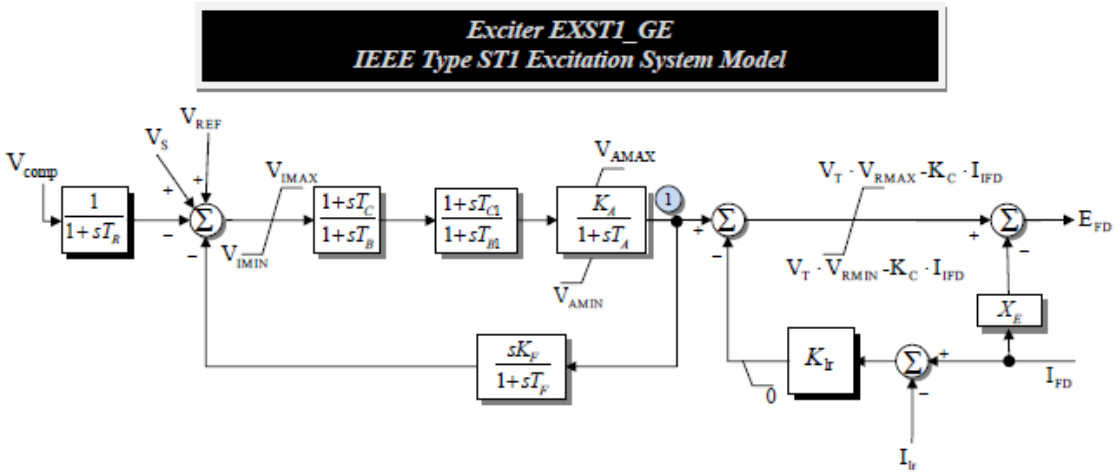

Figure 4.20: Block diagram of EXST1_GE as implemented in PowerWorld [7]

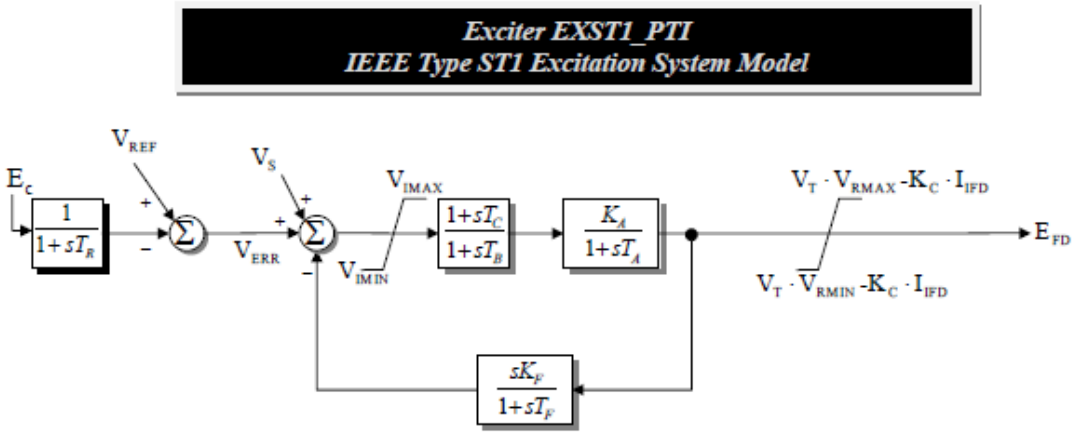

Figure 4.21: Block diagram of EXST1_PTI as implemented in PowerWorld [7]

We chose an example of the SMIB equivalent at Bus 25, Generator 1, derived from WECC Case 4. This generator has a GENROU model, an EXST1_GE model as well as a PSS2A stabilizer. The governor at this generator bus was disabled for the purpose of our study.

In order to run this case in PSSE, the EXST1_GE model was replaced by EXST1_PTI. From Figures 4.20 and 4.21, it is important to note here that the behavior of

these two exciter models will differ, unless there are no limits enforced on *Va* and unless $Tc_1 = Tb_1 = Klr = Xe = 0$.

A solid, balanced, three-phase fault was applied at the generator bus at t = 1 second. The fault was cleared in 0.15 second. A time step of ¼ cycle was used. The results for this case with EXST1_PTI model are as given in Figures 4.22 and 4.23.

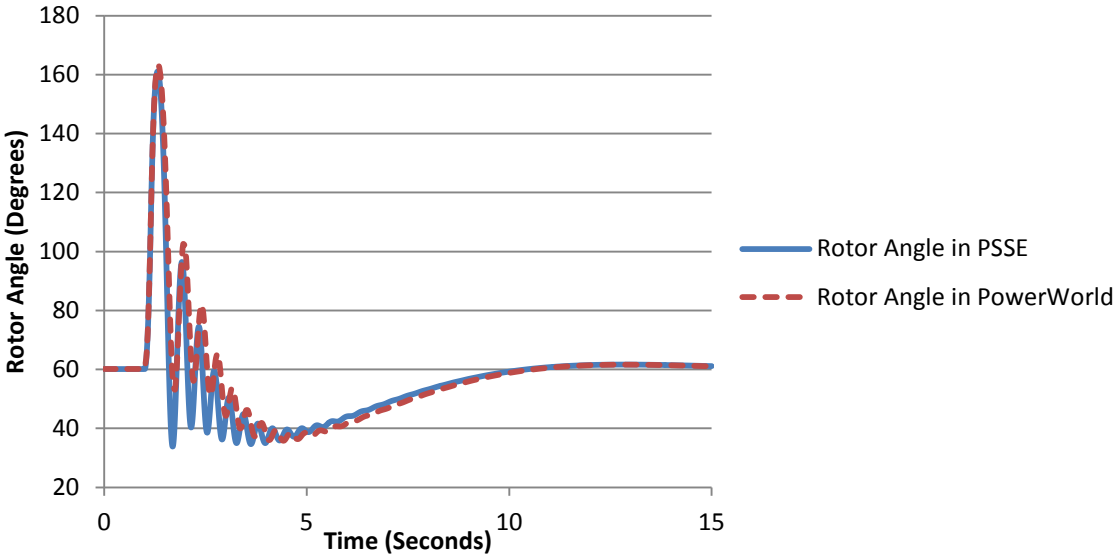

Figure 4.22: Comparison of rotor angles for the case with EXST1_PTI

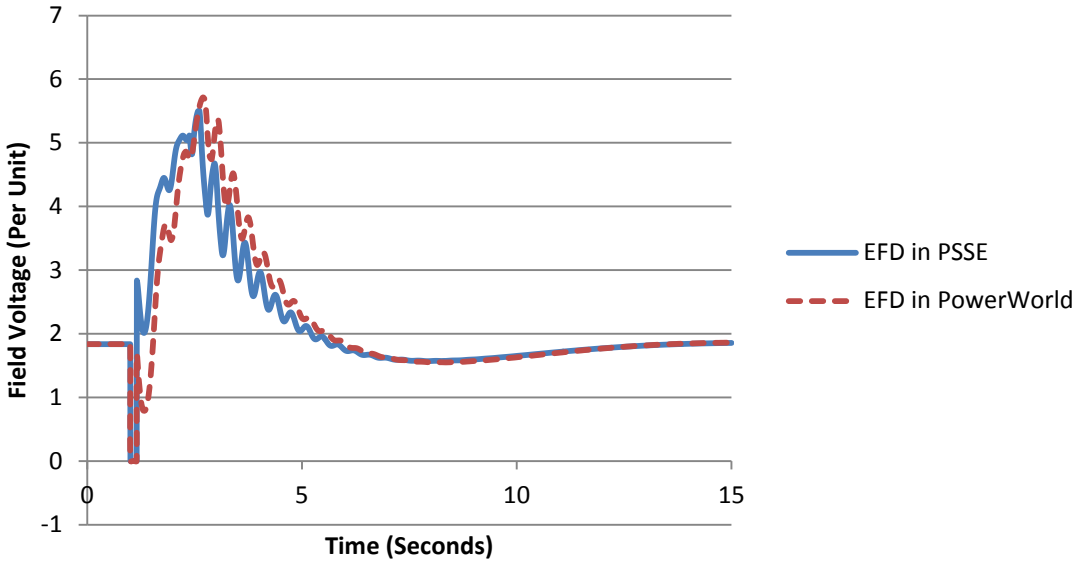

Figure 4.23: Comparison of rotor angles for the case with EXST1_PTI

The errors were due to the fact that, in the EFD limit, PowerWorld was incorrectly multiplying *Vrmax* by the square root of the terminal voltage *Vt* instead of *Vt* itself as it should be from Figure 4.21, page 39. This has now been fixed by PowerWorld.

To validate the PSLF model of this exciter with the PSSE model, we run this case setting a high *Vamax* and low *Vamin* to the PSLF model to account for the lack of the limiter in the PSSE model. A comparison of the results is shown in Figure 4.24.

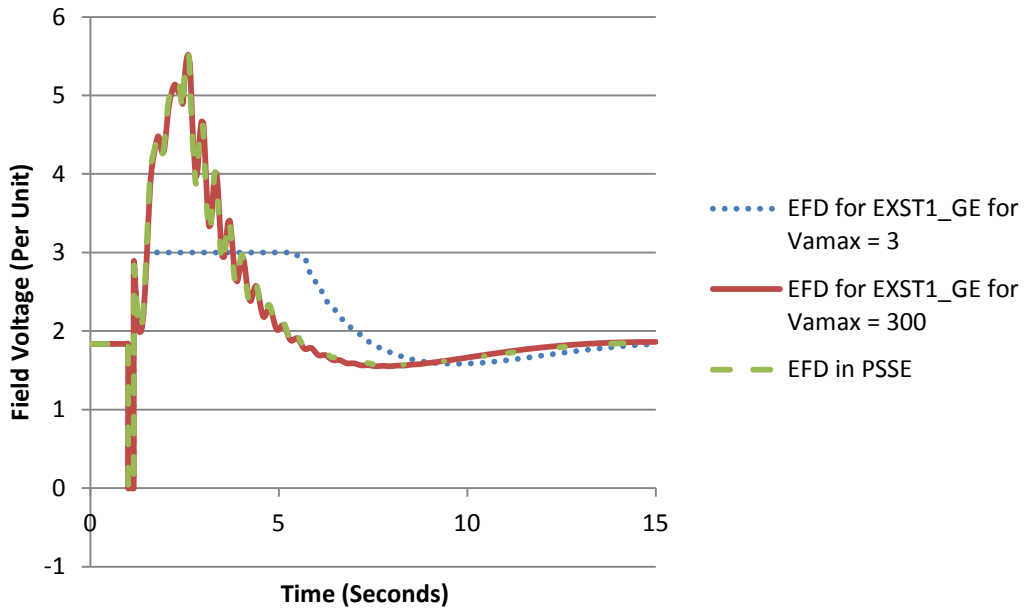

Figure 4.24: Comparison of field voltages for EXST1 GE models with low and very high *Vamax* limits to the field voltage obtained in the PSSE model

From Figure 4.24, note that for a *Vamax* limit set on the PSLF model, EFD gets clipped to *Vamax* if it tries to exceed it.

Thus, we have validated the implementation of EXST1_GE in PowerWorld to EXST1_PTI in PSSE.

In the WECC Case 4, there 869 EXST1 exciters, of which 639 have the *Vamax/min* >= 99, i.e. the limits are set at high values. Hence it is crucial to note that the remaining 230 limits could become active in certain situations. This can lead to discrepant results between the two different implementations that were described here.

4.4 Stabilizer Model Validation

PSS2A – IEEE Dual Input Stabilizer Model: Out of the 1375 stabilizer models present in WECC Case 4, 903 are of the type PSS2A. Hence validation of this model will account for a major part of the stabilizer model validation of the whole system.

To validate this model, we revisit the immediately previous SMIB equivalent created at Generator 1, Bus 25. The same simulation was repeated and the stabilizer outputs were recorded in PSSE and PowerWorld.

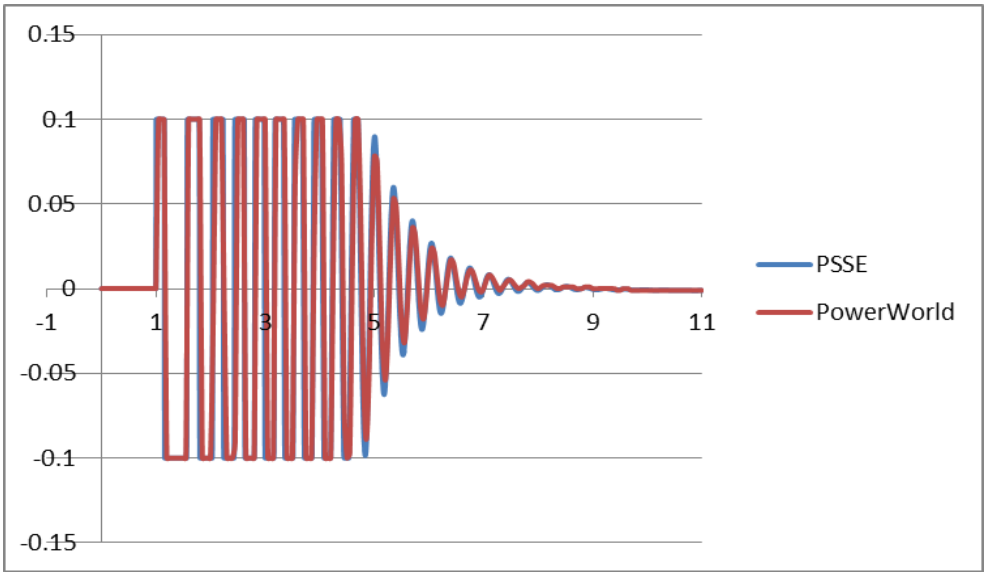

Figure 4.25: Comparison of Stabilizer Signal (VOTHSG) in pu of PSS2A for the SMIB case Gen1, Bus 25

The two signals seem to match reasonably well, as shown in Figure 4.25.

4.5 Key Observations in Botttom-Up Approach

Following are some general observations that were made in the process of this two-bus validation between PowerWorld and PSSE.

4.5.1 Reference Angle

By default PowerWorld uses a center of inertia reference angle whereas in PSSE the reference angle is the internal angle for a generator. Care has to be taken to follow the

same convention of reference angle to achieve proper validation of results of the same system in two different software packages. PowerWorld provides several options to choose angle reference in order to maintain compatibility with other software packages.

4.5.2 Generator Compensation

In PSLF and PowerWorld, generator compensation (*Rcomp* and *Xcomp*) values are modeled as the parameters of the machine model. In PSSE, however, a separate compensation model has to be associated with the machine model where these values can be entered. This was one of the causes of a lot of discrepant results when *.raw and *.dyr files were exported from PowerWorld to PSSE to perform validation. Before making any such comparisons, either *Rcomp* and *Xcomp* should be set to 0 in the machine model in PowerWorld or the compensator model with appropriate values should be added to the machine model in PSSE.

5. Validation of Generator Saturation and Exciter Speed Dependence Using BPA Data

5.1 Validation of Generator Model Saturation Using BPA Data

In the previous chapter, GENROU and GENSAL models were validated between PSSE and PowerWorld using two-bus equivalent systems. Based on the previous analysis these models match quite closely. In this section, the PowerWorld GENROU, GENSAL and GENTPF models were validated with the PSLF models using the generator field current values for a number of BPA generators (at initialization the field current is identical to the field voltage).

Since the initial field current is sensitive to the generator's reactive power output, the first step in the comparison was to determine how closely these values matched. Using the stored generator reactive power outputs for the *.epc input file and the solved PowerWorld case, the match was quite good, but not always exact. For the 2580 online generators in the case, only six had differences above 10 Mvar, 117 above 1 Mvar and a total of 132 above 0.5 Mvar. While the reason for these power flow differences is beyond the scope of the study, it is mostly likely due to differences in how reactive power is shared between generators regulating the same bus.

Without correcting for the power flow reactive power injection differences, there can be substantial differences in the field current that have nothing to do with the transient stability models. For example at the bus 39 generator there is a 9.8 Mvar difference, resulting in a 0.04 per unit field current difference. These differences become more significant for the lower MVA units. To remove this bias, the generator power flow reactive outputs in the PowerWorld case were modified to exactly match the PSLF case values for the 78 BPA units in which the value was above 0.5 Mvars.

In performing the generator field voltage validation, it was noted that sometimes the PSSE and PSLF models gave slightly different results. While the differences were not large (usually less than one percent), they were large enough to require investigation. The result is that the differences appear to be due to a difference between the PSLF and PSSE implementations of generator saturation modeling for the GENSAL and GENROU

models (PSSE currently does not have an equivalent for the GENTPF and GENTPJ models). Both models use a quadratic model in which the amount of saturation is inputted at values of 1.0 and 1.2 (with these saturation values denoted as S1 and S12). For the GENSAL model the saturation is a function of the *Eqp* (the direct-axis transient flux), whereas for the GENROU model it is a function of the total sub-transient flux.

In PSSE the saturation function is explicitly given in the documentation as

$$S(input) = \frac{B_{psse}(input - A_{psse})^2}{input} \tag{5.1}$$

This will be denoted as the scaled quadratic approach. In PSLF the saturation function is not given, but based on numeric testing it appears to be

$$S(input) = B_{GE}(input - A_{GE})^2 \tag{5.2}$$

This will be denoted as the quadratic approach. Since both curves are fit to the same points (1,S[1.0]) and (1.2,S[1.2]), the A and B coefficients are obviously different, as are the S(input) values for inputs other than 1.0 and 1.2. PowerWorld Simulator implements both models, with an option specifying which model to use.

As an example, the generator at Bus 29 is represented using a GENSAL model with S(1.0) = 0.1710 and S(1.2) = 0.9010

Curve fitting the two points gives the following equation for the scaled quadratic approach:

$$S(input) = \frac{9.8057(input - 0.8679)^2}{input}$$

And for the quadratic approach:

$$S(input) = 7.1741(input - 0.8456)^2$$

Figure 5.1 compares the two curves for varying levels of flux; it is readily apparent that both curves correctly pass through the points S(1.0)=0.171 and S(1.2)=0.901. While the difference between the curves is relatively slight, it is not zero. To better illustrate, Figure 5.2 plots the difference between the two using the same x-axis scale as Figure 5.1.

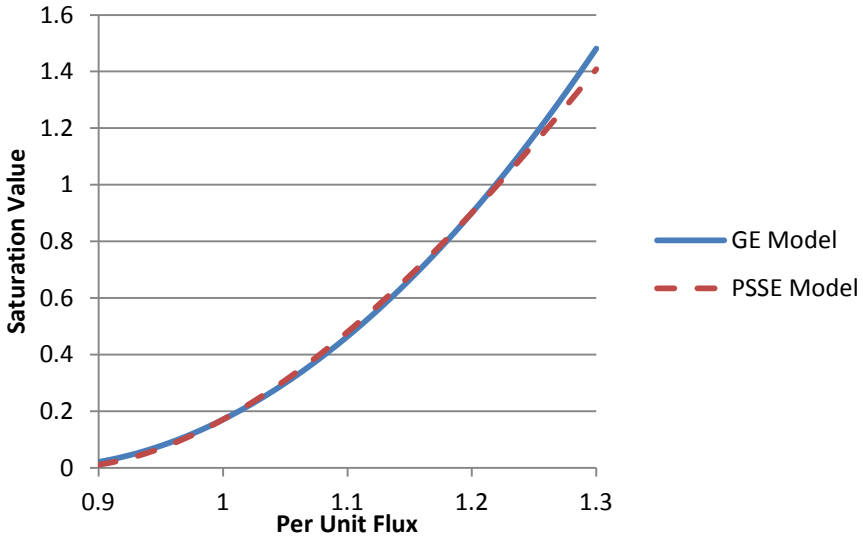

Figure 5.1: Comparison of saturation for scaled quadratic and quadratic saturation functions

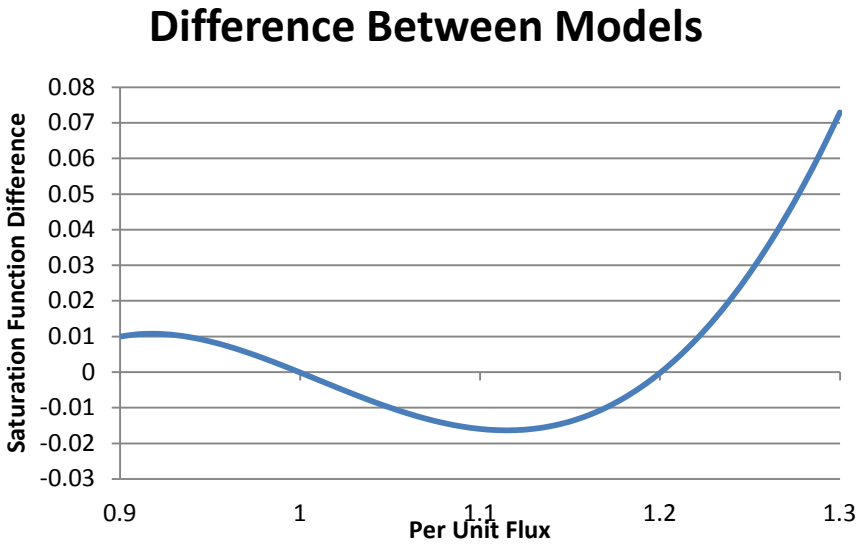

Figure 5.2: Comparison of difference in saturation between PSSE and PSLF functions

The difference in the saturation values for fluxes other than 1.0 and 1.2 results in differences in the field voltage and subsequently in the exciter state variable values. For the bus 29 example, in which the initial per unit flux is 1.051, the scaled quadratic gives an initial field voltage of 2.5137 (based on results using a two bus equivalent) while the quadratic gives a value of 2.5034 (based on results from the WECC Case 4). Note that that -0.0103 difference is quite close to what would be expected from Figure 5.2. The initial field voltage is 2.5147 in PowerWorld when solved with the scaled quadratic saturation modeling and 2.5036 when solved with the quadratic approach, with both values closely matching those from the other two programs.

A second example is for the two generators at bus 30 in which the generator 1 and 2 initial field voltages are 1.6445 and 1.5561 in PSSE and 1.6394 and 1.5506 in PSLF. Solving in PowerWorld, the values are 1.6430 and 1.5543 using the scaled quadratic (PSSE) approach, and 1.6401 and 1.5513 using the quadratic (PSLF) approach; again all closely match.

To validate this approach, the initial field current values for the 200 largest on-line generators (in terms of real power output) in BPA (for which we had data) were compared. Using the quadratic saturation function the average error in the initial field current values was 0.0084 per unit, while with the scaled quadratic saturation function the average error was 0.01223 per unit. If the values are limited to just the 100 largest units, for which small initial differences in the power flow reactive power output would have the least affect, the average was 0.0031 per unit for the quadratic approach and 0.0083 for the scaled quadratic. Since the actual PSLF values were only available with a precision of 0.001, the conclusion appears to be that (1) the PowerWorld software closely matches the initial field values from PSLF, and (2) the quadratic approach is the best way to match the PSLF results.

Since PowerWorld implements both approaches, the significance of the issue can be studied. In the WECC model there are 2533 generators with active generator models. The largest difference in the initial field voltage between the two models is 0.0339 per unit (at the generator at bus 31), with only five generators having differences above 0.03, a total

of 23 having differences above 0.02 and a total of 111 above 0.01 per unit. In terms of percentage, the largest difference is 1.66% at 31, with 25 generators having differences above 1.0%.

This issue is not considered significant, but it does need to be considered during validation between the different packages since differences in the field voltages can get amplified into differences in the initial exciter values.

5.2 Validation of Exciters Using BPA Data

Field Voltage Speed Dependence: After applying the loss of generation contingency as mentioned earlier, the EFD values initially decreased, such as at bus 36. In looking further, this is due to exciter field voltage output being multiplied by the speed. This is something PSLF does on some exciters, but PSSE does not. PowerWorld had this speed effect modeled for some exciters, but not all. This has now been corrected in PowerWorld. Figure 5.3 shows the impact on EFD at Bus 36 (with an EXDC1 exciter), now with a much closer match to PSLF. The initial dip in EFD is caused by declining generator frequency.

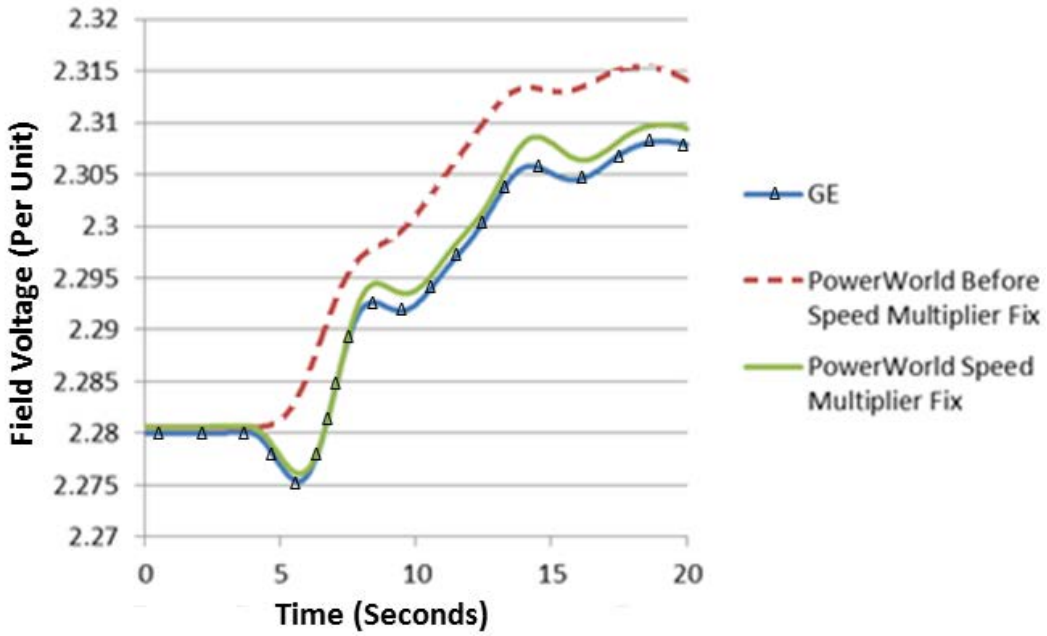

Figure 5.3 : Comparison of EFDs in pu at bus 36 with and without considering speed multiplication factor

6. Time Step Comparisons

Throughout the course of this work, we have mostly used a time step of ¼ cycle since it is the WECC standard. However, in light of the discussion in Chapter 3, it would be interesting to study the system response using different time steps and the corresponding time constant auto-corrections.

In the time step comparison study, we used WECC Case 4. The loss of the same units as simulated earlier was the contingency applied at t = 2 seconds. We used time steps of ¼ cycle and ½ cycle for our comparisons. The simulation was run for a total of 30 seconds.

On "running validation" on this case for each of these time steps, the validation statistics given in Table 6.1 were obtained in PowerWorld.

Table 6.1: Summary of validation messages obtained for WECC Case 4, using different time steps

Time Step ↓	**Validation message fields →**	**Validation Errors**	**Validation Warnings**	**Validation Warnings after Auto-Correction**
¼ cycle		941	41	39
½ cycle		3038	43	41

The large number of validation errors in the instance where ½ cycle is used is intuitive as the most of the time constants of the WECC case must be designed for the standard time step of ¼ cycle. A majority of the auto-corrections consist of those for the time constants, the remaining being reactance and saturation values as discussed in Chapter 2.

The solution statistics using these two different time steps are given in Table 6.2. The network solution statistics are represented by the number of forward/backwards substitutions and Jacobian factorizations.

Table 6.2: Summary of solution statistics for WECC Case 4, using different time steps

Time Step ↓	Solution statistics →	Time to solve	Number of Jacobian Factorizations	Number of Forward/Backward substitutions
¼ cycle		913	73	13725
½ cycle		597	77	9798

Some of the preliminary results obtained from this time step comparison are given in Figures 6.1 to 6.4.

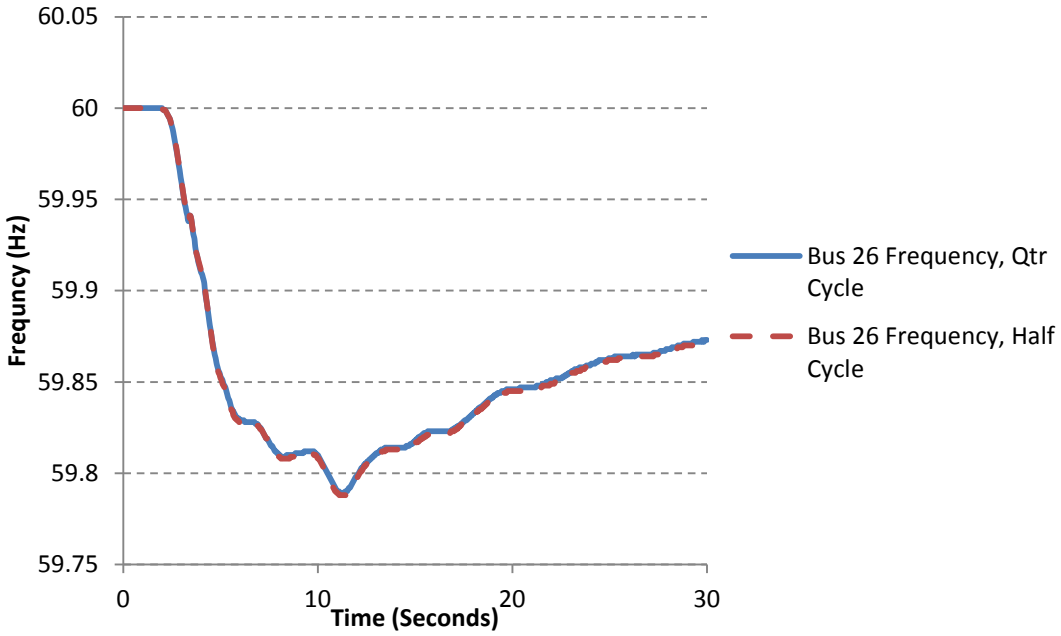

Figure 6.1: Comparison of frequency response at Bus 26 for simulations of different time steps

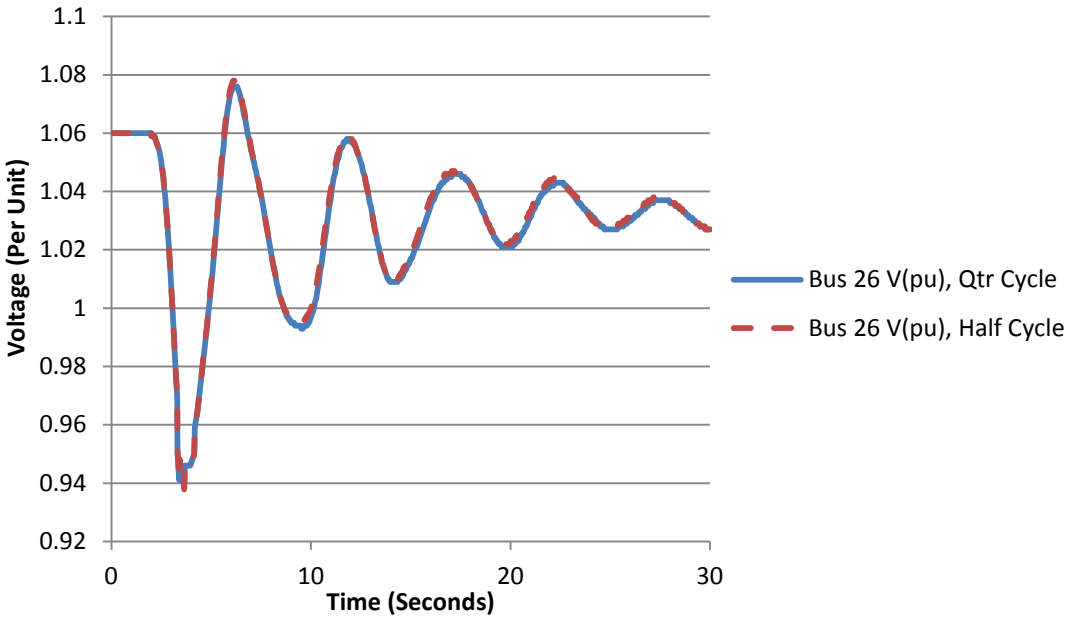

Figure 6.2: Comparison of voltages at Bus 26 for simulations of different time steps

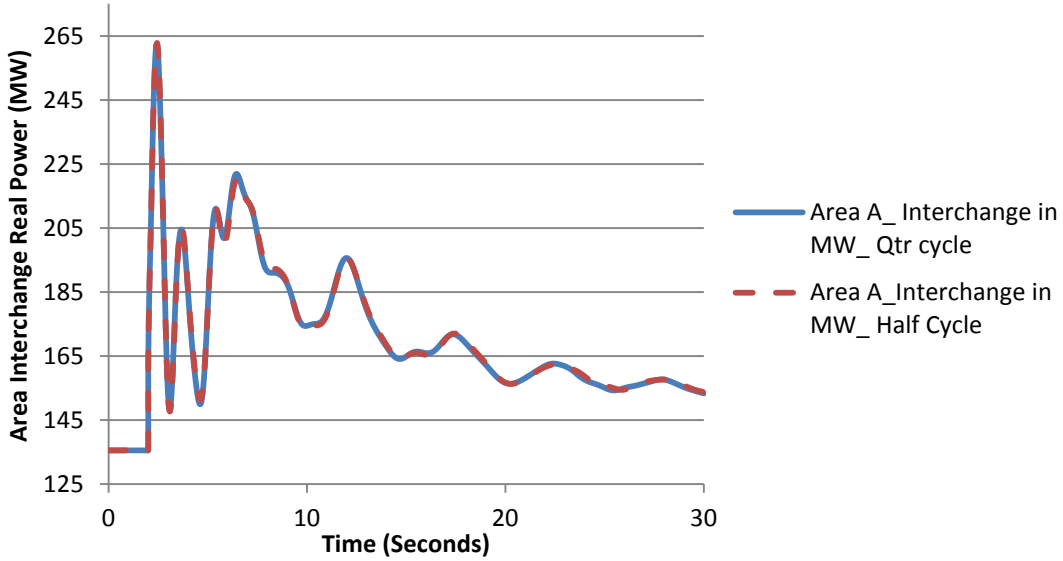

Figure 6.3: Comparison of area interchange in MW for Area A, for simulations of different time steps

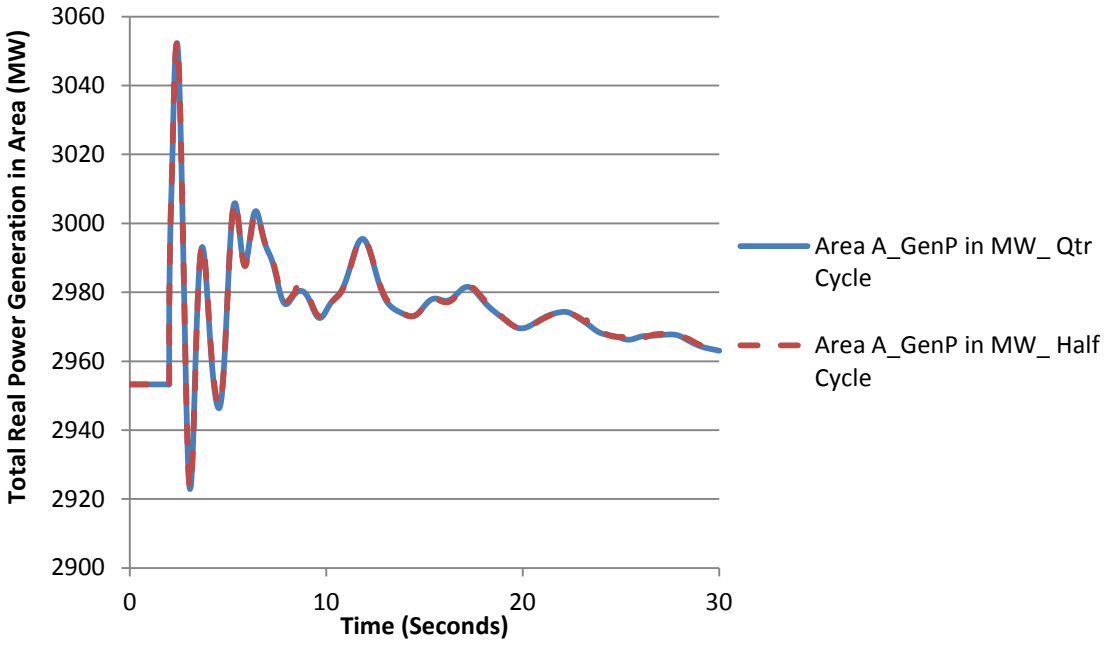

Figure 6.4: Comparison of net generation in MW for Area A, for simulations of different time steps

Such comparisons were repeated for several buses, generators and areas and we found that for simulating the whole 17,000 bus system, changing the time step and the subsequent auto-corrections in PowerWorld did not make a significant difference in the results. Thus it is probably safe to assume that changing the time step within a certain acceptable range for the stability and accuracy of the simulation will not have much of an impact on the results.

7. Frequency Comparisons of WECC Case 4

7.1 Overview

This chapter covers the comparison of results between PowerWorld (version 16 beta) and PSLF (version 17) for WECC Case 4, consisting of 17710 buses and 3470 generators. The tested scenario is the loss of the same generating units, as studied earlier. For the simulations, the system was initially allowed to run unperturbed for two seconds to demonstrate a stable initial contingency. Then the contingency was applied at time t = 2.0 seconds and the simulation run for a total of 30 seconds. Both cases were integrated using a ¼ cycle time step.

7.2 Frequency Comparison

During the simulation the bus frequencies, as shown in Table 7.1, and voltages were modeled at 20 locations selected by BPA to give a representation for system behavior.

Table 7.1: Final frequencies at the specified 20 buses at the end of 30 seconds

	Bus Number	**Final frequency in PowerWorld (Hz)**	**Final frequency in GE (Hz)**
1.	26	59.873	59.862
2.	27	59.872	59.867
3.	40	59.877	59.851
4.	41	59.875	59.853
5.	42	59.872	59.864
6.	43	59.872	59.865
7.	18	59.869	59.862
8.	44	59.873	59.858
9.	11	59.872	59.865
10.	45	59.872	59.867
11.	46	59.875	59.855
12.	47	59.872	59.859
13.	48	59.872	59.864
14.	49	59.872	59.865
15.	50	59.872	59.864
16.	51	59.872	59.867
17.	52	59.877	59.850
18.	53	59.872	59.867
19.	54	59.877	59.850
20.	55	59.873	59.859

The bus frequency response is compared for five different locations in the system in Figures 7.1 to 7.5, with increasing distance from the contingency location. With the exception of Figure 7.5, the figures show a fairly good correlation in the frequency response, with all recovering to roughly the same 30 second frequency value. The initial drop in frequency, roughly to about 59.9 Hz, is almost identical in all the figures. This phase corresponds to the inertia response of the generators, indicating that both packages have quite similar inertia representations for the generators. The final frequency recovery value is determined by the droop settings on the governors that are allowed to respond to under frequency events. That the final values appear to be converging indicates that these values are probably modeled correctly.

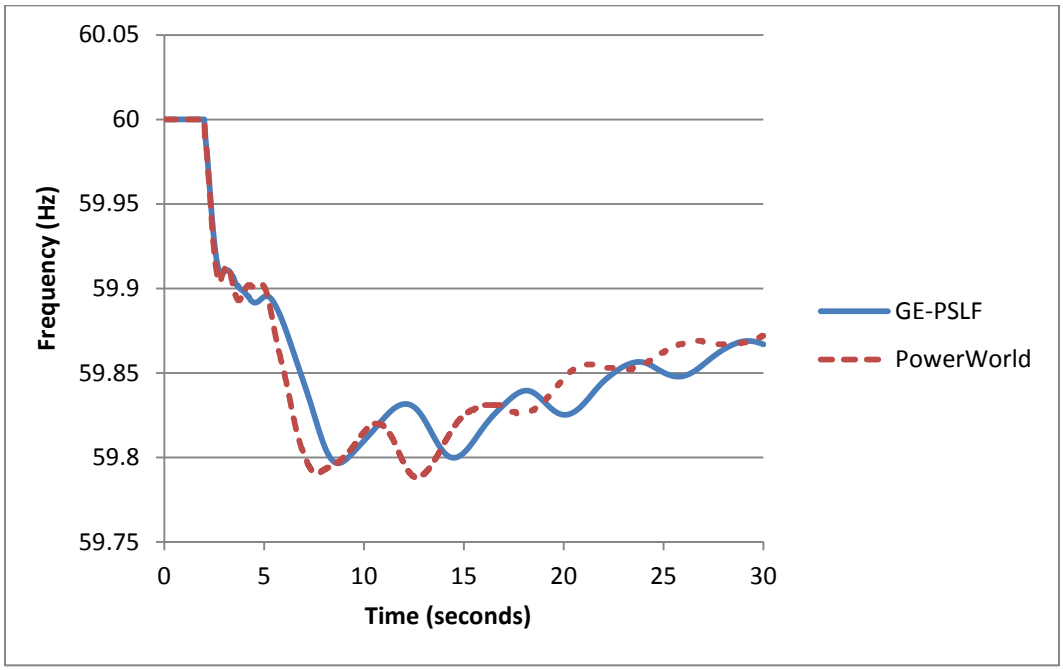

Figure 7.1: Frequency comparison at Bus 45

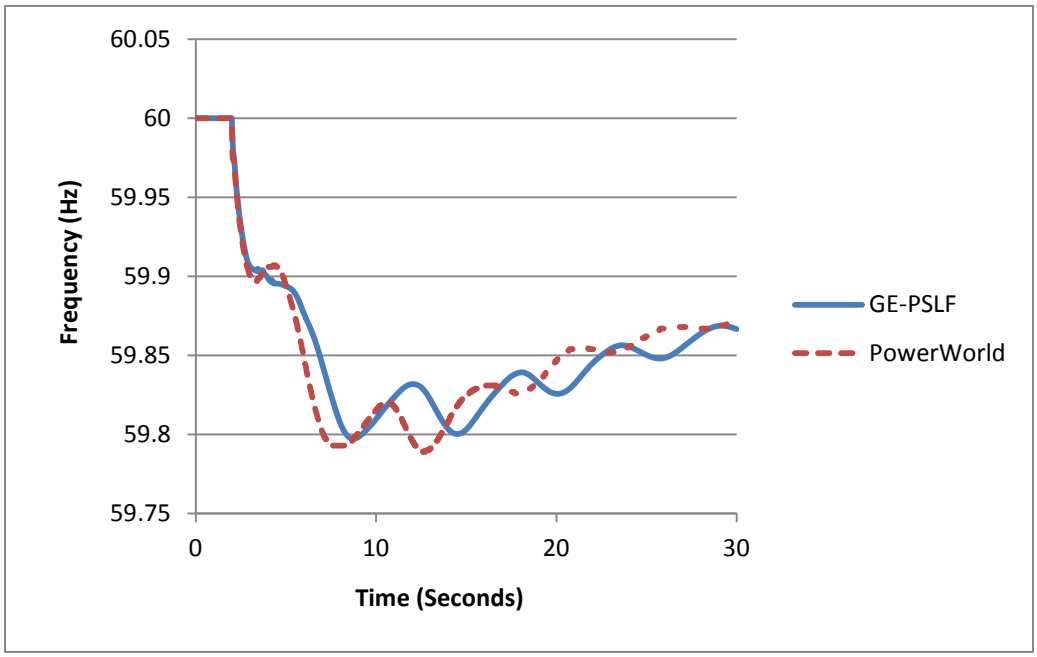

Figure 7.2: Frequency comparison at Bus 27

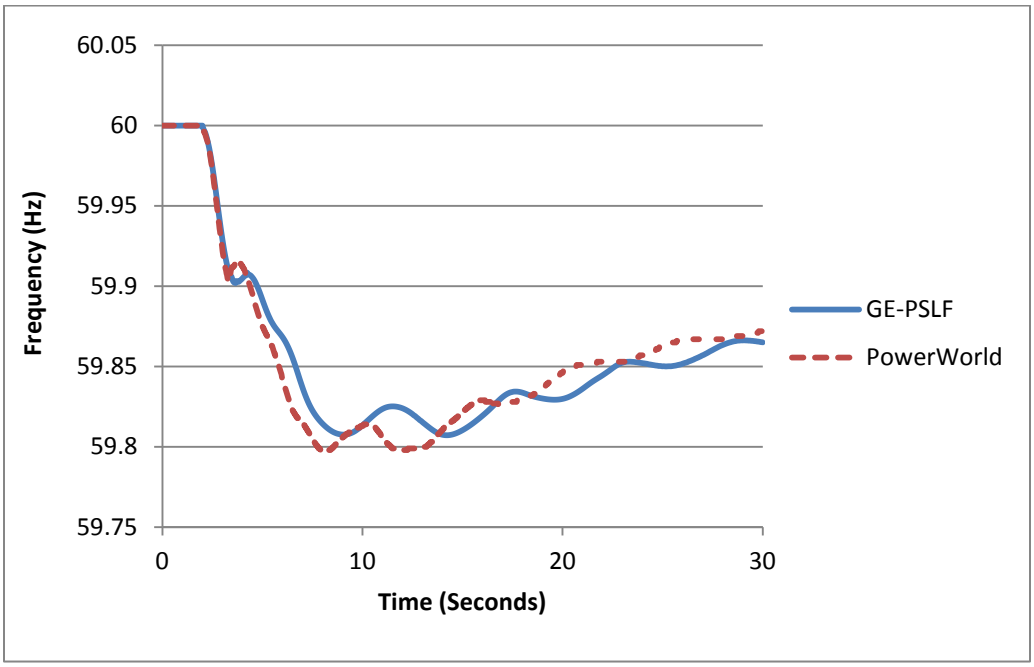

Figure 7.3: Frequency comparison at Bus 43

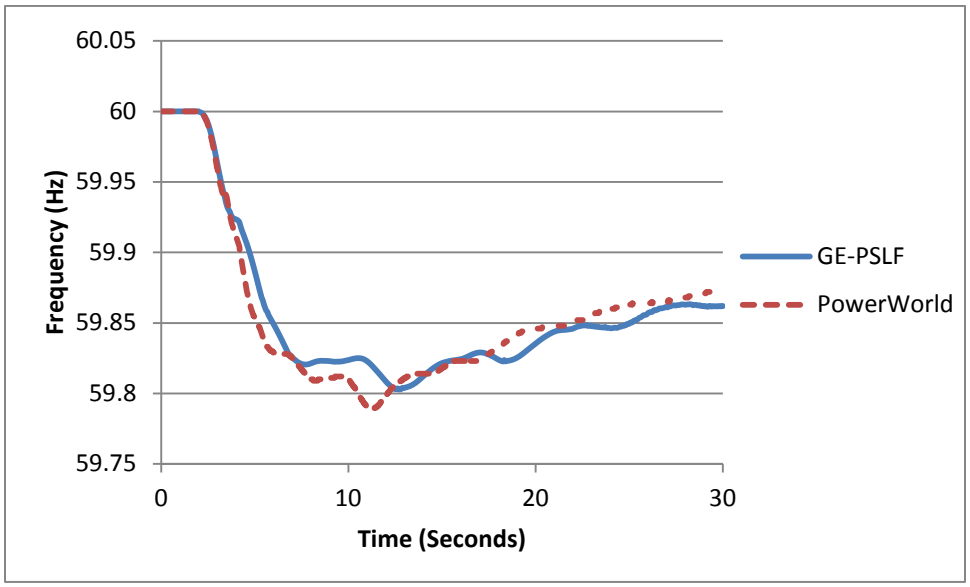

Figure 7.4: Frequency comparison at Bus 26

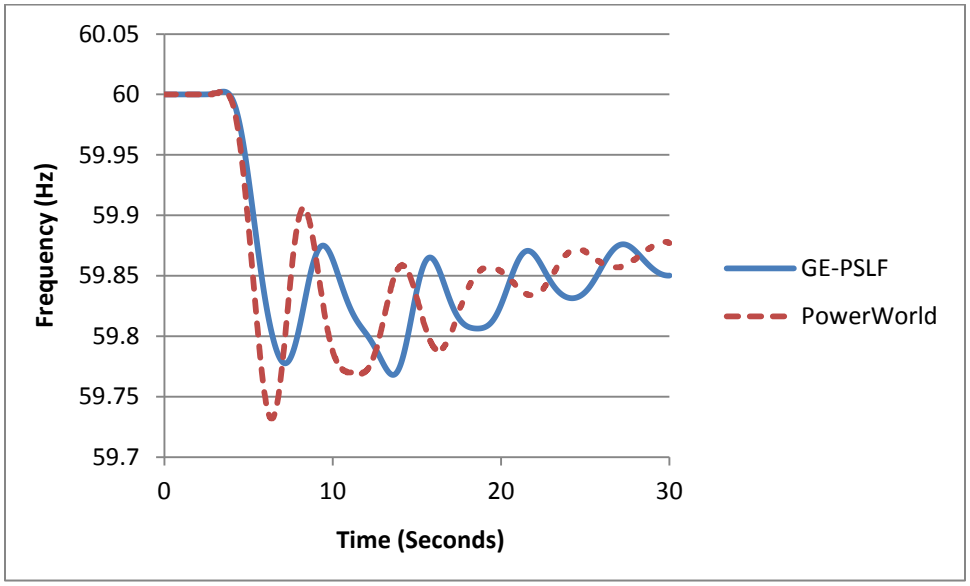

Figure 7.5: Frequency comparison at Bus 37

The most significant difference in all five figures is that PowerWorld has a slightly quicker decay in the frequency, and its lowest frequency is lower than that for PSLF. While this is most significant for bus 37, it is present to a lesser extent at the other buses as well.

The frequency response difference, especially in the region of Bus 37, is a major concern. After some trial and error techniques, it was found that some of the issues were arising due to the dynamic load models. To verify this, all the dynamic load models in the case were simplified and converted to real power-constant current and reactive power-constant impedance type loads. The system was subjected to the same simulation and some improvements in the results were obtained, as seen in Figure 7.6 and 7.7.

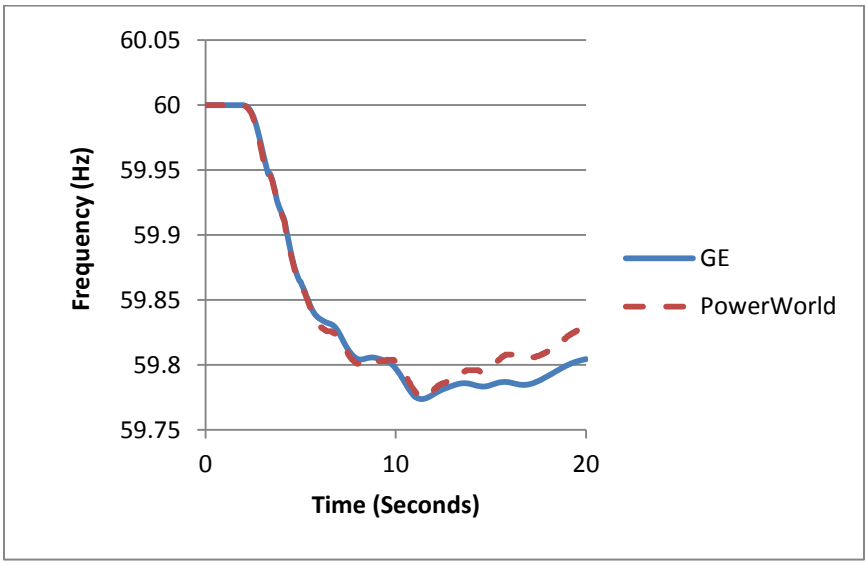

Figure 7.6: Bus 26 frequency response with PIQZ load showing improved results

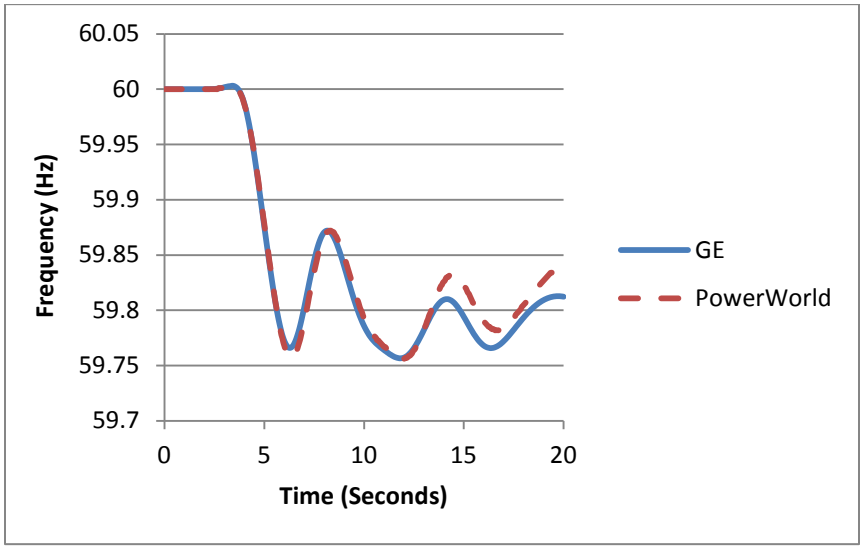

Figure 7.7: Bus 40 frequency response with PIQZ load showing improved results

However, there were still some voltage variations at Bus 40, as shown in Figure 7.8, pointing to the fact there might be an inherent voltage issue here.

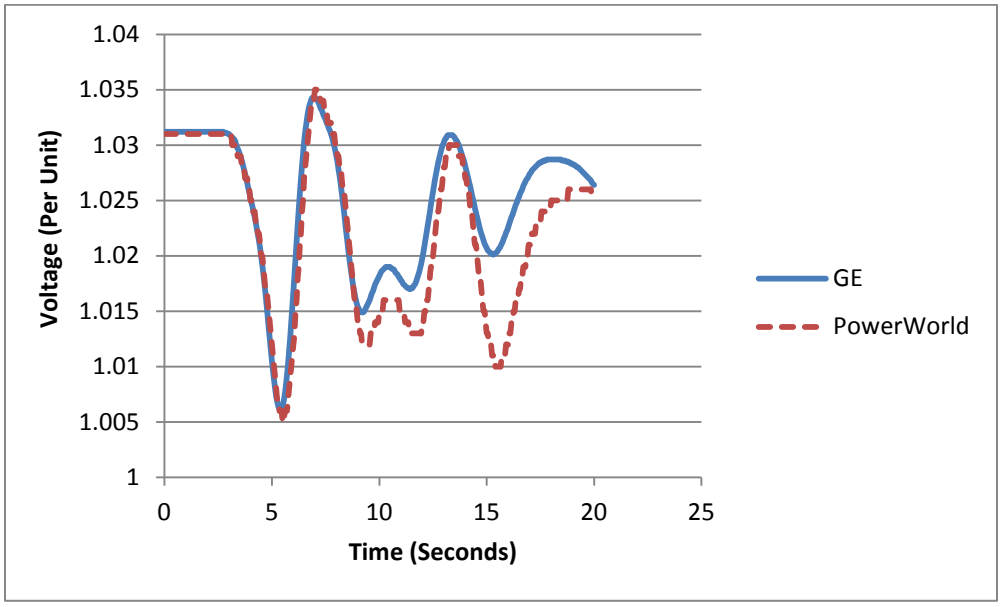

Figure 7.8: Bus 40 voltage comparisons with PIQZ load

After delving more into the governor model GGOV1, an error was found in PowerWorld associated with the GGOV1 load limiter module. Figure 7.9 shows the mechanical power output of the largest active generator in Area A before and after this change, compared to GE. However, despite the prevalence of the GGOV1 models in the WECC system, this change did not have a significant impact on the frequency errors we encountered, particularly after 15 seconds, as shown in Figure 7.10.

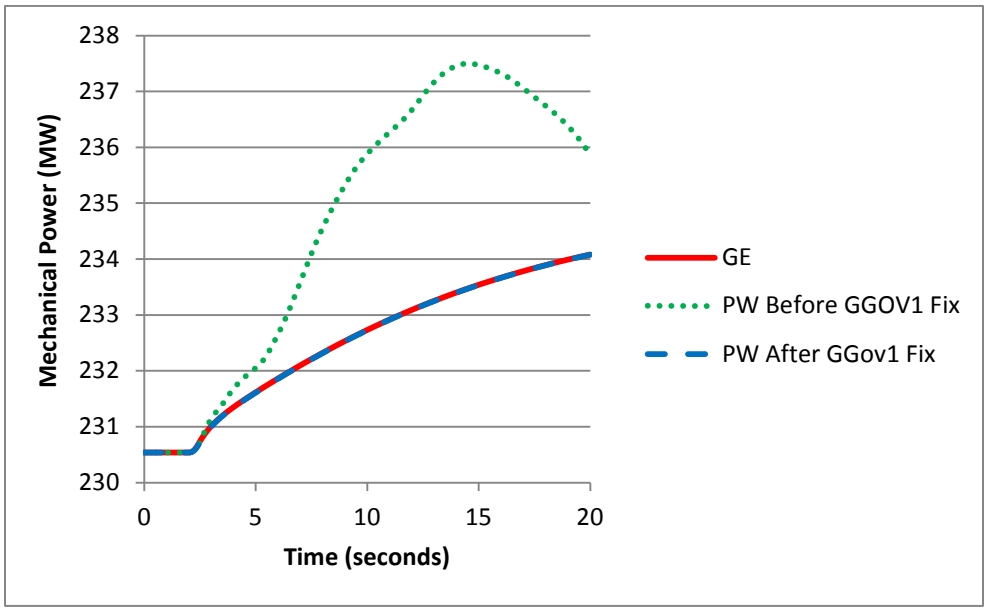

Figure 7.9: Comparison of mechanical power output of largest active generator in Area A

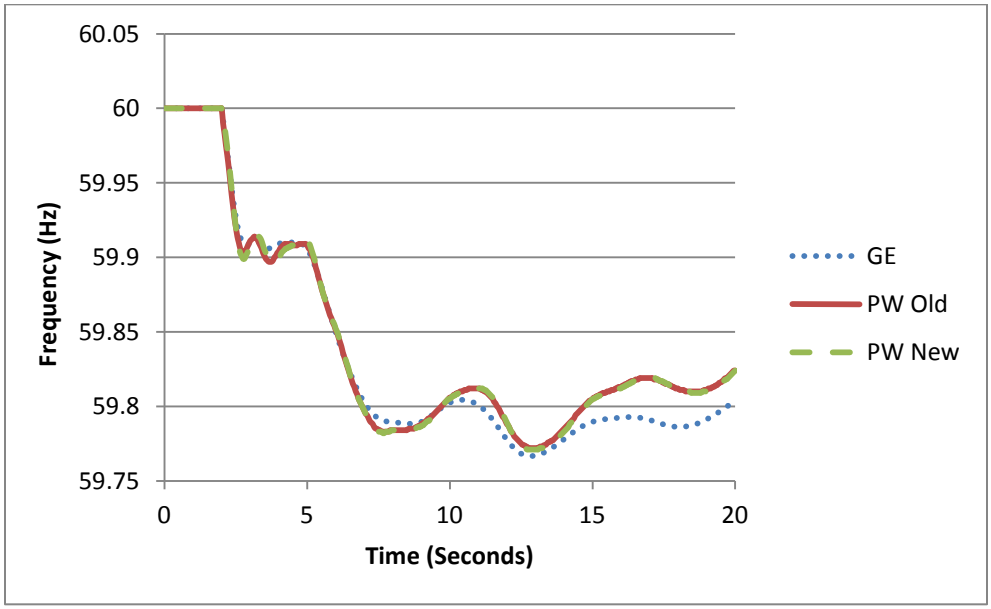

Figure 7.10: Frequency response after rectifying GGOV1 errors

There are still issues as far as the frequencies are concerned. At the culmination of this work, we are still left with figuring out the reasons behind these discrepancies. This leads to a direction for future work.

8. Summary and Directions for Future Work

We have presented and implemented a methodology to validate transient stability models used in power systems. Although we focused on the generator and its associated models, our methodology is scalable and can be used on systems of various sizes and for different types of dynamic models such as load models.

From the vast differences in results obtained for essentially the same system and similar models across different transient stability packages, this work also highlighted the need for validation or software packages, transient stability models as well as results.

In Chapter 7, we concluded that we need to further investigate the reason for the difference in frequency responses. There might potentially be more issues with some of the softwares we used here that probably need more testing and analyses similar to the ones charted out in this thesis

Another direction would be to try and automate these comparisons and the whole validation process, both top-down and bottom-up, to handle the huge volumes of data and get meaningful results quickly and efficiently.

Given the research thrust on increasing the penetration of renewables in the grid, validation of dynamic models pertaining to wind turbines, solar models, etc., is also another avenue that can and should be pursued

Additionally, a logical future step would be to validate these packages and their simulation results with real-world data obtained from phasor measurement units (PMUs), digital fault recorders (DFRs) and other sensing devices.

References

[1] P. Kundur, *Power System Stability and Control*, New York, NY: McGraw-Hill, Inc., 1994.

[2] V. Vittal, "Transient stability test systems for direct stability methods," *IEEE Transactions on Power Systems,* vol. 7, February 1992, pp. 37-42.

[3] K. K. Kaberere, K. A. Folly and A. I. Petroianu, "Assessment of commercially available software tools for transient stability: Experience gained in an academic environment," in *IEEE Africon 2004*, vol. 2, September 2004, pp. 711-716.

[4] K. K. Kaberere, A. I. Petroianu, and K. A. Folly, "Is there a need for benchmarking power system stability simulation tools?" in *Proceedings of the 16th Power Systems Computation Conference,* July 2008, pp. 1-7.

[5] K. K. Kaberere, K. A. Folly, M. Ntombela, and A. I. Petroianu, "Comparative analysis and numerical validation of industrial-grade power system simulation tools: Application to small-signal stability," in *Proceedings of the 15th Power Systems Computation Conference,* August 2005, session 32, paper 3, pp. 1-7.

[6] A. V. Ubisse, K. A. Folly, K. O. Awodele, and D. T. Oyedokun, "Comparison of Matlab, PST, PSAT and DigSILENT for transient stability studies on parallel HVAC-HVDC transmission lines," in *Proceeding 45th International Universities Power Engineering Conference,* 2010, pp. 1-6.

[7] PowerWorld Simulator block diagrams. (June 2010). [Online]. Available: http://powerworld.com/Document%20Library/version.150/Block%20Diagrams.pdf

[8] PSS/E™ 30 Program Application Guide: Volume 2, Power Technologies, Inc. (2004). [Online]. Available: http://www.cadfamily.com/download/EDA/PSSE-Power/PAGV2.pdf

[9] WECC Approved Dynamic Model Library. (September 2006). [Online]. Available: http://www.wecc.biz/committees/StandingCommittees/PCC/TSS/MVWG/111306/Lists/Minutes/1/Approved%20Models.pdf